Simulation-based analysis of flight schedules at tactical planning level

C. Răducanu

Technische Universiteit Delft

TU Delft

Simulation-based analysis of flight schedules at tactical planning level

by

C. Răducanu

to obtain the degree of Master of Science
at the Delft University of Technology,
to be defended publicly on 28 of February 2020 at 10:00 am.

Student number:	4347560	
Project duration:	April 16, 2019 – February 28, 2020	
Thesis committee:	Dr. M. A. Mitici,	TU Delft, Responsible thesis supervisor
	Dr. B.F. Santos,	TU Delft, Committeee Chair
	Dr. F. Oliviero	TU Delft, Examiner

TU Delft

Contents

List of Figures

List of Tables

Nomenclature

Abbreviations

4DT	4D trajectory
A/C	Aircraft
AH	Airborne Holding Delay
AHP	Analytical Hierarchy Process
ANSP	Air Navigation Service Provider
APM	Aircraft Performance Model
ATC	Air Traffic Control
ATCo	Air Traffic Controller
ATFCM	Air Traffic Flow and Capacity Management
ATFM	Air Traffic Flow Management
ATM	Air Traffic Management
BADA	Base of Aircraft Data
BDT	Business Development Trajectory
BT	Business Trajectory
CAS	Calibrated Airspeed
CASA	Computer Assisted Slot Allocation
CDM	Collaborative Decision Making
CI	Cost Index
CoO	Contract of Objectives
CTA	Controlled Time of Arrival
DCB	Demand and Capacity Balancing
DDR2	Demand Data Repository 2
EPS	Ensemble Prediction Systems
ETA	Estimated Time of Arrival
ETO	Estimated Time Over
EUROCONTROL	European Organization for Safety of Air Navigation
EWF	Ensemble Weather Forecasts
FDM	Flight Dynamics Model
FPL	Filed Flight Plan
FMS	Flight Management System
GH	Ground Holding Delay
HIL	Human-in-Loop
I4D	Initial 4D Trajectory Management
ICAO	International Civil Aviation Organisation
ILP	Mixed Integer Linear Programming
LLC	Low-cost Carriers
LNAV	Lateral Navigation
MILP	Mixed Integer Linear Programming
NextGen	Next Generation Air Transportation Systems
NMOC	Network Manager Operations Centre
OCC	Operation Control Centre
PT	Predicted Trajectory
RBT	Reference Business Trajectory
RPL	Repetitive Flight Plan
RTA	Required Time of Arrival
SBT	Shared Business Trajectory
SESAR	Single European Sky ATM Research

SWIM	System Wide Information Management
TBO	Trajectory-based Operations
TIGGE	THORPEX Interactive Grand Global Ensemble
TW	Time Window
UI	User Interface
VNAV	Vertical navigation

List of Symbols

h	altitude
$t_{arrival}$	arrival time at waypoint
ϕ	bank angle
ψ	heading angle
d	distance between two subsequent waypoints
D	aerodynamic drag
C_D	drag coefficient.
d_{turn}	minium distance to start the turn onto the next flight-leg
C_F	fuel coefficient
F	fuel consumption
g_0	gravitational acceleration
φ	latitude
L	aerodynamic lift
C_L	lift coefficient.
λ	longitude
M	Mach number
m	aircraft mass
m_{ref}	time
R_{turn}	radius of turn
$t_{scheduled}$	scheduled flight time
ρ_0	sea level air density in standard atmosphere
a_0	speed of sound in standard atmosphere
$t_{closing}$	TW closing time
t_{ERR}	time error
t_{ETA}	estimated time of arrival
T	thrust
C_T	thrust coefficient
t	time
$\frac{d}{dt}$	time derivative
t_{input}	time input for the target speed calculation
$t_{opening}$	TW opening time
$t_{schedule}$	scheduled flight time
η	thrust specific fuel consumption
t^{TW}	time corresponding to a simulation with the TW type
V_{CAS}	calibrated airspeed
V_{GS}	ground speed
V_{TAS}	true airspeed
V_w	wind speed

1 Introduction

1.1. Background

Demand for air transportation has been growing since the industry-wide deregulation back in the 1970s, proving resilient to external shocks along the way, such as the Gulf Crisis, 9/11 or the 2008 Financial Crisis. [1] forecasts expect the average revenue passenger per kilometer (RPK) to increase with 4.4% per year over the next 20 years, which means that in 15 years world traffic is going to double. Three key drivers support the increase in air traffic: airline business models, economic and income growth and the development in infrastructure and technology.

Due to the growing worldwide market presence of *Low-cost Carriers* (LLC), which have 49% and 29% percent of the market share in Europe and the US respectively, airfares have dropped by 0.9% per year over the past ten years (from [3]), boosting passenger demand. The focus of LLC airlines on point-to-point, short-haul operations, using only a fleet of single-aisle aircraft, has forced legacy carriers to broaden their airline networks to increase connectivity and points served. This business model will continue to stimulate growth in the coming years.

As a result, airspace are becoming more and more congested, and the modernization of the current ATM system is needed to maintain the safety level of the transportation system and to increase the capacity and flight efficiency. [42] found that the main inefficiencies of the European ATM system are: fixed routes and airspace structures, which do not allow aircraft operators the freedom to fly their preferred trajectory, surveillance and trajectory prediction technology, which do not permit aircraft to fly with the *four-dimensional* (4D) navigation precision they are equipped with and finally, flight delays due to high traffic areas. The SESAR ATM modernization programme was developed to accommodate the air traffic growth in Europe. [10] envisions that the new ATM system will accommodate double the annual number of Instrument Flight Rules (IFR) flights, reduce the cost of ATM services by 50% for airspace users and increase the safety level per flight by three times.

The concept of TBO is fundamental to the future ATM system, as defined by the SESAR research project. At the core of TBO is the *4D trajectory* (4DT), which consists of a set of points defined in time and space, which represent the flight path of the aircraft. TBO enables all ATM stakeholders: airlines, airports and *Air Navigation Service Provider* (ANSP), to have the same view of the aircraft trajectory, through the 4DT such that the flight can be operated as close as possible to the airline's ideal flight path, while ensuring that a range of ATM functions are being carried out, such as demand-capacity balance of airspace sectors and conflict management [27]. The benefit of TBO is that it increases the predictability of the aircraft trajectory by having stakeholders share information in the early planning stages.

In the current ATM planning framework, airlines get to submit their final fight schedules hours before operation. This means demand and capacity imbalances in the ATM network are only dealt with tactically though a process known as ATFM. It optimizes the flow of air traffic in time and in space, such that the total delay in the system is minimized. There is an extensive set of optimization models and tools developed over the past 20 years [2] that support ATFM. TBO supports the development of similar network optimization methods at a strategic and pre-tactical level to develop optimal fight schedules that solve for demand-capacity imbalances in the airspace sector in an effort to deal with limiting factors in the network early on.

1.2. Problem Statement

Strict adherence to the 4DT time constraints set at a strategic level (typically six months in advance) may not be feasible in a system as complex as the European ATM. Uncertainties or inaccuracies about operations are inherent and therefore the optimal flight plan is constantly changing over time as the day of operation approaches and more information becomes available. On the other hand, complete flexibility to Airspace Users would reduce the efficiency of the ATM network which would conflict with the Airspace Users business goals. Therefore, the balance between predictability and flexibility in ATM network planning is crucial to meet the demands of all stakeholders in TBO [27].

A proposed method to balance predictability and flexibility is to create strategic and pre-tactical plans which are capable of absorbing uncertainty due to the appearance of foreseen events through the temporal element of the 4DT. Instead of imposing a fix time constraints at sector entries, which is the typical approach in ATFM [6, 14], the fourth dimension in TBO is modelled as a temporal interval called a *Time Window* (TW) [9].

The network benefits of TW is that it increases predictability within the system, while allowing for some flexibility and possibility of delay absorption. However, how much flexibility this provides to airspace users and how these strategic and pre-tactical constraints impact the aircraft performance in the tactical phase remains unknown. This is in part due to the limitations of the modern *flight management system* (FMS) algorithm. Although the *Flight Management System* (FMS) can support time adherence to one time constraint along the trajectory with an accuracy of several seconds [15], it cannot support contiguous time constraints, neither does it allow aircraft to adhere to time intervals. Hence, in order to evaluate the strategic and pre-tactical network schedules in the tactical phase, a speed control algorithm that permits aircraft to adhere to TW should be developed.

1.3. Research Questions, Aims and Objectives

The first aim of the research is to develop a TW control algorithm and use it to perform a flight-centric evaluation of the strategic and pre-tactical network schedules through simulations of operation. To determine the feasibility of TW, this new algorithm must permit aircraft to adjusts their speed to meet contiguous time intervals during flight.

The objective is to asses the aircraft performance when the aircraft is required to adhere to TW constraints when flying, to determine if the models used to assign TWs can facilitate TBO through integration of the schedules into the *Network Operations Plan* (NOP) and serve as a basis for stakeholder collaboration.

Based on the gaps in literature identified trough a literature review and the research framework, the main research question becomes:

What type of time constraints should aircraft adhere to along their trajectory, that satisfy both ATM network constraints and yield a balance between fuel consumption and flight time of an individual flight?

In the process of answering the primary research question, the following sub-questions are propose:

1. (a) How to develop a speed control methodology that has aircraft adhere to time constraints along the aircraft trajectory?
   (b) How can the speed control methodology be evaluated with respect to the flight time and fuel consumption performance of each individual aircraft in the atm network at a tactical level?
2. (a) What type of tactical air traffic uncertainty source should be considered when evaluating the adherence to time constraint of a flight?
   (b) How can the uncertainty sources be modelled in the evaluation?
3. (a) What type of flight metrics should be used when evaluating the performance of the optimized flight schedules?

The assessment is to be performed with respect to individual flight punctuality and fuel consumption by means of a simulation of the operations. The product of the assessment is a comparison between the different types of tools that generate time constraints such that the method that is conductive to trajectory-based operations is established. In this case conductive refers to the model that would require the least tactical time shift in the time constraints from the planned one while maintaining a balance in fuel consumption.

1.4. Report Structure

The structure of this report is as follows: Part I presents the scientific paper in which the questions presented above are answered. Part II continues with the literature review that was conducted in preparation for the research undertaken. Chapter 2 presents the TBO concept of operations and the on-board technology that it most relies on, the FMS. The different mathematical modes in which time constraints are imposed and the different types of time constraints are presented in Chapter 3. In Chapter 4 the uncertainty sources considered in strategic and pre-tactical planning are outlined and the main sources of uncertainty in ATM network discussed. The role of the simulation environment in the flight-centric tactical assessment of time constraints is outlined in Chapter 5. Finally, in Part III an elaboration on the thesis work is given by explaining in detail the simulation environment used in Appendix A and the fuel consumption estimation in Appendix B.

I

Master of Science Thesis Paper

Simulation-based analysis of flight schedules at tactical planning level

Author MSc Student: Claudia Răducanu[a],
Supervisors: Mihaela Mitici[a], René Verbeek[a]

[a] *Faculty of Aerospace Engineering, Delft University of Technology, Delft, The Netherlands*

Abstract

This paper analyzes flexible flight schedules at the tactical level of air traffic flow management from the aircraft performance point of view. Flexible flight schedules are four-dimensional trajectories in which the temporal constraint is a time interval, called a time window (TW), in which aircraft are required to arrive. The larger the width of a TW the higher the flexibility the aircraft has to perform its flight. To evaluate the flight schedules, we compared the fuel consumption and time adherence of 20 trajectories when flying under flight schedules with different level of flexibility. For the analyzes, we developed a TW control logic that requires aircraft to adjust their speed throughout the flight if the arrival time is not within the time bounds of a TW. Our results showed that flexible flight schedules allow for fuel saving as long as the delay encountered by a trajectory is not larger than the TW width. Results also revealed that there is a limited number of speed changes required to maintain an aircraft along the flexible flight schedule. However, the phase of flight planning during which the TWs are developed does not have an impact on the flight performance. It is only the degree of flexibility offered by the TWs that matters. From a flight performance perspective, this study emphasizes the fuel benefit of flexible flight schedules during the tactical phase.

Keywords: time windows, tactical assessment, strategic planning, BlueSky ATM simulator

1. Introduction

Due to the growing demand for air travel over the past decade, there is an immediate need to tackle the inefficiencies in the air traffic management (ATM) system to maintain the safety level of the transportation system. These range from fixed routes and airspace structures, to a high degree of flexibility in flight planning available to airlines. In the current operational context, the airline must submit their final flight schedules hours before the operation, while the sector capacities are allocated months in advance based on historical air traffic demand assessments [13]. This means that aircraft have to operate in an environment in which there are inherent demand and capacity imbalances. The proposed solution by SESAR and NexGen ATM modernization programs is to increase the predictability of the system through early information sharing between ATM stakeholders: airlines, airports and air navigation service providers. This is achieved through a shift in operational paradigm, from airspace-based operation to trajectory-based operations (TBO). The core of TBO is the 4D-trajectory, which is an accurate description of the aircraft path in time and space (latitude, longitude, flight level and time). The 4D-trajectory is continuously shared and updated between all ATM stakeholders during all planning phases improving predictability in the ATM system while maintaining efficiency [9].

To support early information exchange for network flight planning in TBO, recently a set of methods that generate network flight schedules which satisfy demand and capacity imbalances have been developed for a range of planning phase. These methods presented in [1, 6, 5] have focused on the adaptation of air traffic flow management (ATFM) models for use at strategic, months before operation, and pre-tactical, seven to one day before operation, planning phases. The network flight schedules consist of 4D-trajectories assigned to aircraft that satisfy demand and capacity in the ATM network.

When imposing 4D constraints along the trajectory, there needs to be a balance between the priorities of the ATM network and those of airlines [12]. Strict adherence to a static baseline defined in one of the early planning stages limits the flight efficiency enabled by the airborne systems. On the other hand, providing Airspace Users (AU) with total flexibility to define their flight plans as in the current context, reduces the network efficiency, and also has an impact on the AU operations. Therefore, the strategic or pre-tactical flight planning have to allow for flexibility

while simultaneously maintaining predictability. One proposed method is planning with tolerance levels on the four dimensions of the trajectory. Since the use of target times is key to TBO, [4] have proposed modeling the temporal dimension of the 4D-trajectories as a time interval, also called a time window (TW). The width of the TW indicates the amount of flexibility that airlines have during flight execution. The concept of operations requires aircraft to remain within the TWs along the trajectory to avoid demand and capacity imbalances within sectors. The advantage of the TW concept of operations is that it strengthens the decision-making role of airlines within the ATM process. [5].

In this paper, we address the challenge of evaluating the impact of the TW concept of operations on individual flight performance during the tactical phase of air traffic flow management. This phase takes place a couple of hours before the flight operation. The flight time and fuel consumption needed to adhere to the TWs are under consideration. For the tactical assessment, we propose a control model based on speed adjustments that allow aircraft to track contiguous TWs placed at critical waypoints along the trajectory.

The remainder of the paper is structured as follows. In Section 2, we discuss the mathematical models that assign TWs to flights taking into account en-route capacity constraints and uncertainty sources that can affect the arrival punctuality of aircraft. The discussion continuous with the methodology in Section 3, where we introduce the TW control loop and outline the reseach structure. Finally, Section 4 presents the results of the flight-centric tactical assessment, followed by the discussion in Section 5.

2. Background

A TW is a period of time during which the aircraft is required to take-off, land or enter into a sector in the trajectory. It is characterized by an opening time $t_{opening}$, which represents the earliest possible time to complete the action, and by a closing time $t_{closing}$, which represents the latest possible time to complete the same action. The $t_{opening}$ corresponds to the scheduled take-off, landing and sector entry times and hence define the position of the TW, while the $t_{closing}$ defines the TW width or the degree of flexibility available to the flight. The smaller the TW width, the more important it is for the entire air traffic system that the flight is executed as close as possible to the scheduled flight plan. Figure 1 shows the TW concept of operations. The line from the aircraft to the $t_{opening}$ indicates the scheduled trajectory of the aircraft, while the line connecting the aircraft and the $t_{closing}$ shows the maximum path deviation from the scheduled trajectory that the aircraft is allowed to be on. The figure shows that the actual aircraft trajectory, in red, crosses the TW position between the two TW bounds. This means that the aircraft maintains a speed schedule that has it arrive within the bounds of the TW.

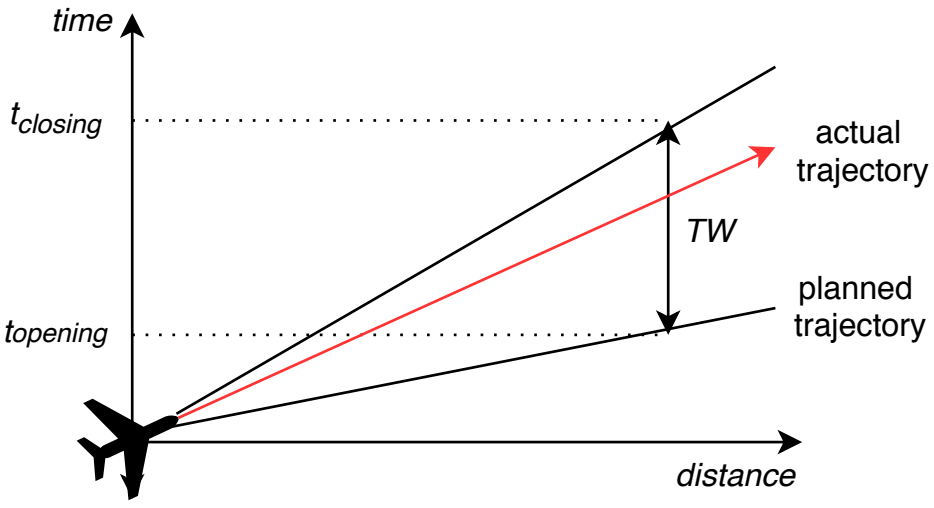

Figure 1: Illustration of the time window concept of operations.

In literature, mathematical models that assign TWs to flights are proposed for both the strategic (six months to seven days before the day of operations) [3, 5] and the pre-tactical (six days to one day before the day of operations)

[16] planning phase. The TW models aim to maximise the total duration of all TWs, thus looking for the maximum flexibility for the flights in the system while respecting en-route capacity constraints. These are defined as the number of entries into the sector during an hour. A TW is composed of a discrete and limited number of contiguous time periods of fixed width of 1 min. The maximum width of the TW is 15 min. The formulation of Corolli et al.[5] defines both the position and width of the TW through a bi-objective mixed-integer linear programming model . First the model determines the sets of TWs that minimise the total cost of delay and then selects the set in which the total width of the existing TWs is maximised. The second step was necessary in order to offer the ATM stakeholders the maximum flexibility in their operations. However, the model proved computationally expensive.

The formulation of Castelli et al. [3] relies on the solution of a strategic flight distribution model [1] to fix the opening times of the TW and then tries to maximises the total duration of all TWs. The strategic flight distribution model takes as input the scheduled flight plans by airlines, which do not consider airspace capacities, and it proposes possible shifts from the schedule that satisfy the associated capacities. The range of possible shifts consist of a change in either the take-off or landing time. In the end the assigned trajectories minimise either the total shift or operational costs across all flights. Using the computed take-off time, the times of entry into sectors along the trajectory and finally the landing time, the integer-linear programming model of Castelli et al. [3] identifies the TW widths.

The pre-tactical model of Mitici et. al [16] is an extension of the strategic model of [3] that takes into account probabilistic sector entry times due to uncertainty in the weather conditions to fix the TW widths. This model makes use of information that becomes available at the pre-tactical phase, to update the TW widths such that they offer the highest degree of flexibility allowable to airlines leading to a better utilization of resources, more robust plans and a more efficient support for ATM controllers and stakeholders. The solution of the pre-tactical TW model in comparison to the strategic solution [3] shows a decrease in the number of narrow TWs for the same flight schedules. In addition, under 1% of the TW shrink under the pre-tactical solution.

3. Methodology

In this paper, we evaluate the impact that the TW concept of operations has on the individual flight performance during execution through fast-time simulation of operation. A comparison is made between the flight performance of aircraft in the tactical phase when they have to adhere to: i) scheduled flight plans without TWs ii) scheduled flight plans with TWs assigned through the strategic model [3] iii) scheduled flight plans with TWs assigned through the pre-tactical model [16] iv) scheduled flight plans with relaxed TWs.

The flight schedules with TWs are generated in the strategic or pre-tactical planning phases, when there is uncertainty about the tactical air traffic environment. To understand how these uncertainty sources affect the fuel consumption and generate en-route deviations from the flight schedules in the tactical phase, they must be modelled in the simulation environment. In this research, to capture the tactical air traffic environment, we model two major sources of uncertainty: i) the wind conditions and ii) departure delays.

The four types of flight schedules with assigned TWs, the wind conditions and departure delays make up the independent variables of this research and are assumed to be the most influential. Other influential factors that are not directly considered are the trajectory, the aircraft type and the aircraft weight. However, there no scenario are created to ensure an exhaustive range of these other factors.

For the simulations, we propose a TW control system that allows for aircraft operation within a given time window via velocity control. Whenever the estimated time of arrival (ETA) of a flight is within the TW opening and closing time, the aircraft maintains its prevailing speed. When the ETA is outside the TW bounds the speed is adjusted accordingly to meet the time constraint. Subsequently, the output of the simulation is analysed for fuel consumption

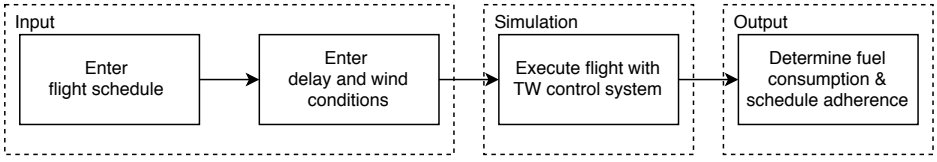

Figure 2: Overview of the research methodology.

and the adherence to the flight schedules. An overview of the methodology is provided in Fig. 2. The following paragraphs describe the chosen data for this research, the set-up of the TW control system and the analysis method in detail.

3.1. Flight schedules data

The scheduled flight plans are available from the DDR2 database [10], which contains historical traffic data, including: traffic demand, last filed flight plans (M1 files) as well as actual flown trajectories (M3 files). As described in Section 2, the input to the strategic and pre-tactical TW models are the set of last filed flight plans (M1 files in DDR2) redistributed at the strategic planning phase to satisfy capacity constraints using the model of Bolic et. al [1]. Table 1 shows the structure of such a flight schedule that is used as input for the two TW models. It consists of an ordered list of waypoints which the aircraft must follow from the departure to the arrival airport. Each waypoint is defined by its geographical coordinates, latitude and longitude, and can be located at the same place as a navigation-aid. The flight schedule contains a planned cross-over time and flight level for each waypoint.

Table 1: A sample of an aicraft flight schedule used as input for the TW model.

AC ID	Waypoint ID	Flight Level	Time Over Geopoint	Order	Latitude	Longitude
AEA1517	GONIM	360	11/02/2017 19:32:00	24	44.45	2.84
AEA1517	MEN	360	11/02/2017 19:34:00	25	44.61	3.16
AEA1517	NINUN	360	11/02/2017 19:37:00	26	44.77	3.56

The tactical evaluation of the TW concept of operations takes as input the scheduled flight plans, such as the one in Table 1, along with the TWs obtained thought the strategic and pre-tactical model for the same flight plans. Figure 3 presents the 20 flight plans considered for the tactical assessment. Along the vertical axis there is the flight ID and corresponding to each ID there is a horizontal line whose length indicates the duration of the scheduled flight time of the cruise level-off phase. The markers on the line indicate the position of the TWs (opening times) assigned to waypoints in the flight plan by the models in Section 2. Not all waypoints present in a flight plan were assigned a TW, but only a limited set of interest for each flight. For the remaining waypoints the "Time Over Geopoint" is discarded.

The factor that has the largest influence on the aircraft performance when required to adhere to a flight schedule with TWs is the type of TW. In this study, we use four types of TW assigned to the scheduled flight time described in Figure 3 to evaluate the flight performance of aircraft when flying under the TW concept of operations. This leads to four separate flight schedules for each flight evaluated. The first two flight schedules are the flight schedules with TWs obtained using the strategic model [3] and the flight schedules with TWs obtained using the pre-tactical model [16]. These two types of schedules represent the scenario in which the aircraft is flying under TW concept of operation. The third type of flight schedule represents the scenario in which the aircraft is flying using required times of arrival (RTA). For this we impose a TW with a width of 1 minute at each TW postion described in Figure 3. We consider this the most limiting scenario in which the aircraft has to operate. Finally, we introduce the most flexible scenario in which the aircraft would have to operate: 60 minute TW along all TW positions. In the remaining of the paper, we refer to the flight schedules with their associated TW types as: strategic, pre-tactical, the 1 min and the 60 min TWs. The length of the TWs for a specific flight is the same along all constrained waypoints in it's path. In Table 2, the strategic and pre-tactical TWs assigned to each trajectory are presented, along with the flight level of the cruise phase and the initial speed of the aircraft which is calculated as the average speed between the first two waypoints of the cruise phase.

3.2. Uncertainty modelling

There are several sources of uncertainty that may affect the aircraft arrival punctuality in a sector such as: data uncertainty, operational uncertainty, equipment uncertainty and weather uncertainty [21]. The flight schedules described in Section 3.1 are developed in time-frames where there is still a lot of doubt about the conditions on the day of the operations. To understand the robustness of the flight schedules, any information that is known about the air traffic system tactically must be used in the concept evaluation. In this study, we consider analyzing wind related uncertainties, as reliable forecasts are available several days to hours before the flight execution day and departure delay uncertainties as they are expected to induce significant deviations from the flight plans.

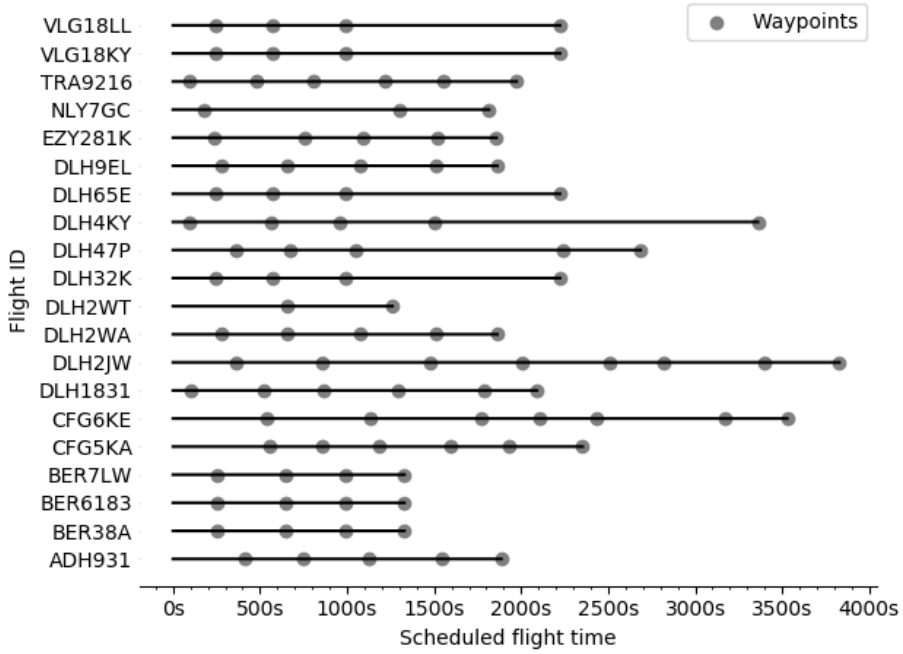

Figure 3: Scheduled flight time $t_{scheduled}$ for the flights selected in the tactical assessment of the TW concept of operation.

Table 2: Specifications of the trajectories selected for the tactical assessment of the TW concept of operations.

AC ID	**Aircraft Type**	**Strategic TWs** min	**Pre-tactical TWs** min	V_{CAS} (kts)	$V_{CAS,max}$ (kts)	**Flight Level**
ADH931	A320	10	15	258	273	350
BER6183	A320	6	15	310	350	240
CFG5KA	A320	10	15	271	285	340
CFG6KE	A320	10	15	258	273	360
DLH1831	A320	10	15	247	260	380
DLH2JW	A321	4	15	264	280	350
DLH32K	A320	10	15	247	261	380
DLH47P	A321	3	15	271	286	340
DLH4KY	A320	10	15	247	261	380
DLH65E	A320	10	15	247	261	380
DLH9EL	A319	10	15	300	350	230
EZY281K	A319	6	15	241	255	390
NLY7GC	A321	10	15	258	273	360
TRA9216	B737	10	15	247	261	380
BER38A	A320	10	15	310	350	240
VLG18LL	A320	10	15	247	261	380
DLH2WA	A319	10	15	300	350	230
BER7LW	A320	10	15	310	350	240
DLH2WT	A320	6	15	283	299	320
VLG18KY	A320	10	15	247	261	380

3.2.1. Departure delay

The departure time uncertainty is modelled as a uniform ground delay of the aircraft for several minutes. We assume that the delay propagates to the first waypoint of the flight cruise phase resulting in the late arrival by the same amount of time. For each trajectory, four different lengths of ground delay were explored: i) five, ii) ten, iii) fifteen, iv) twenty minutes For each combination of TW type described in Section 3.1 and delay value a simulation is carried out to understand the flexibility that TWs provide in aircraft operation and how much delay can be absorbed by the TWs in the tactical phase.

3.2.2. Wind conditions

A major source of uncertainty both in strategic and pre-tactical planning phase is the wind profile on the execution date. In air traffic management literature, Ensemble Prediction Systems (EPS) have been used in order to study the predictability of flight plans and sensitivity to weather uncertainty [11, 20, 16]. The main characteristic of an EPS is that it runs the same numerical weather prediction model with slightly different initial conditions or different parametrization of physical processes to produce a set of 10 to 50 different forecasts called "members" of the ensemble.

In this study, we use an ensemble weather forecast containing 50 forecasts to model the wind profile in the simulation environment used for the tactical assessment. Each of the 20 trajectories, described in Section 3.1 , is simulated using the 50 ensemble members. The wind data used comes from the THORPEX Interactive Grand Global Ensemble (TIGGE) project from the ECMWF model [2]. Each forecast is produced with slightly perturbed initial conditions and has the same likelihood of occurring of $\frac{1}{50}$. Since, the simulation are carried out at a tactical level, we use ensemble forecasts with a lead time of one day from operations.

The wind data for each ensemble member (i) is provided by the ECMWF model as a wind vector, whose magnitude is determined by two parameters: the northward wind vector $V^i_{w,n}$ and the eastward wind vector $V^i_{w,e}$. The parameters are available on eight pressure levels and on a spacial grid defined by 0.5deg east-west resolution and 0.5deg north-south resolution. This translates to 360 equally spaced latitude lines between the pole and the equator, with a line of latitude at the equator and a spacing of 0.5deg between each line. On each latitude circle there are 360 longitude points, starting from 0deg and separated by 0.5deg. The data has a temporal resolution of 6 h from the forecast release time. Therefore, the two wind components of wind for each ensemble member (i) are a function of latitude (φ), longitude (λ), pressure level (p) and time (t) as described by Eq. (1).

$$V^i_{w,n} = f(\varphi, \lambda, p, t) \qquad \mathrm{V}^i_{w,e} = f(\varphi, \lambda, p, t) \tag{1}$$

$$\tag{2}$$

The wind components $V^i_{w,n}$ and $V^i_{w,e}$ along the predicted path are used to determine the relative ground speed of the aircraft. From the data structure described above, the wind components are obtained through multivariate spline interpolation of the first order of the four variables ϕ, λ, p, t of the wind data. The probabilistic flight punctuality at TWs along the trajectory is determined by taking into account the spread of each wind speed component. The northward $V^{i*}_{w,n}$ and eastward $V^{i*}_{w,e}$ wind speeds are calculated using Eq. (3), where $\bar{V}_{w,n}$ and $\bar{V}_{w,e}$ are the average northward and eastward components over the 50 ensemble members.

$$V^{i*}_{w,n} = V^i_{w,n} - \bar{V}_{w,n} \qquad V^{i*}_{w,e} = V^i_{w,e} - \bar{V}_{w,e} \tag{3}$$

$$\bar{V}_{w,n} = \frac{1}{50}\sum_{i=1}^{50} \bar{V}_{w,n} \qquad \bar{V}_{w,e} = \frac{1}{50}\sum_{i=1}^{50} V^i_{w,e} \tag{4}$$

Finally, Eq. (5) defines the aircraft ground speed during the trajectory simulation using ensemble member (i), where V_{TAS} is the true airspeed of the aircraft and ψ is the heading angle.

$$V^i_{GS} = \sqrt{(V_{TAS}\cos\psi + V^{i*}_{w,n})^2 + (V_{TAS}\sin\psi + V^{i*}_{w,e})^2} \tag{5}$$

3.3. Simulation Development

In this section the simulation details are outlined including: the simulation platform, the fuel consumption module used and the TW control system developed for the assessment.

3.3.1. Simulation Platform

The BlueSky Open Air Traffic Simulator developed at TU Delft is used to explore the effect of introducing strategic TW constraints in the tactical phase. The simulator is open source and works under the GNU General Public License v3.0. The simulator has a wide range of features, which also counts a flight management system (FMS) function that facilitates the lateral (LNAV) of the aircraft. For a full account of BlueSky capabilities refer to [14]. The fast-time simulations of operations are performed on a laptop with a 2.6 GHz Intel Core i7 processor and 16 GB 1600 MHz DDR3 RAM. The TW control system presented in Section 3.3.3 was used in this study to asses the impact on the flight performance of the TW concept of operation. The system was implemented within the BlueSky simulator and made compatible with the LNAV function of the simulator. The traffic situation defined by the DDR 2 flight plan and TW is reconstructed in BlueSky using input files (.scn) containing a time-stamped list of commands.

3.3.2. Calculating fuel consumption

BADA models the aircraft kinematics through the Total-Energy Model (TEM) in Eq. (6), based on the forces acting on the aircraft: lift, drag D, thrust T and weight. The other equation in the BADA Motions model is Eq. (7), which describes the change in the aircraft mass along the trajectory, where F is the fuel consumption, measured in $\mathrm{kg\,s^{-1}}$, m is the aircraft mass and dt is the simulation step in the fast-time simulation environment.

$$T - D = mg_0 \frac{dh}{dt} + mV_{TAS} \frac{V_{TAS}}{dt} \tag{6}$$

$$m = -\mathrm{F}dt \tag{7}$$

To asses the impact of TWs at the tactical level from the aircraft performance point of view the flight schedules from Section 3.1 are simulated. The trajectories are simulated using the Base of Aircraft Data (BADA) 3.0 [17] and the open-source BlueSky simulator. For these flights, the fuel consumption must be determined. BADA 3.0 has it's own fuel consumption model, however it has some limitations as the fuel consumption F is only dependent on thrust and not altitude and the relation between thrust and airspeed for turbofan engines is neglected. Since speed changes are the enabling mechanisms of the TW concept of operations, their impact on the flight performance cannot be captured through the BADA 3.0 fuel consumption model.

The mathematical model of BADA 4.0 is better at capturing the physical dependency of the fuel consumption on the thrust and altitude, especially for turbofan engines. Therefore, in this study the Base of Aircraft Data (BADA) 4.0 [18] fuel consumption model is used. The model requires as input the following information about the aircraft state to determine the fuel needed to cover a distance: the aircraft mass m, the altitude h, the true airspeed V_{TAS}, the bank angle ϕ and the horizontal acceleration $\frac{dV_{TAS}}{dt}$.

Using the aircraft state information obtained as a result of the fast-time simulations of operations performed in BlueSky with BADA 3.0, the fuel is obtained using BADA 4.0. The independent use of the BADA 4.0 fuel model has been used in literature in cases where the level of accuracy requested by the application is high [19]. The Propulsive Forces Model (PFM) of BADA 4.0 offers a separate fuel model for each of the three engine types: turbofan, turboprop and piston. In all cases, the fuel determination procedure requires the calculation of the aircraft actions: weight, lift, drag and thrust using the BADA 4.0 Actions model.

The general formula for the fuel consumption F is as follows [18]:

$$\mathrm{F} = \delta \cdot \theta^{\frac{1}{2}} \cdot m_{ref} \cdot g_0 \cdot a_0 \cdot \mathrm{L}_{\mathrm{HV}}^{-1} \cdot C_F \tag{8}$$

Here, δ is the pressure ratio, θ is the temperature ratio, $\mathrm{m_{ref}}$ is the reference mass, from the PFM, g_0=9.806 65 $\mathrm{m\,s^{-2}}$, a_0 is the speed of sound at sea level, $\mathrm{L_{HV}}$ is the fuel lower heating value and C_F is the fuel coefficient. For each engine type and flight phase there is a different method to determine the C_F. In this study all flight are carried out with a turbofan engine, for which the engine rating is [18]:

$$C_F = \begin{cases} C_{F,idle}, & \text{when idle rating is used} \\ \max(C_{F,gen}, C_{F,idle}), & \text{when non-idle rating} \\ & \text{or no rating is used} \end{cases} \tag{9}$$

where, $C_{F,idle}$ is the idle thrust coefficient and $C_{F,gen}$ is the general fuel coefficient, used either in the case of non-idle ratings such as maximum climb (MCMB) and maximum cruise (MCRZ), or in the case of direct throttle parameter input. The former parameter is a function of Mach number and atmospheric conditions as defined by Eq. (10), while the later is a function of the Mach number and thrust coefficients C_T as defined by Eq. (11). The thrust coefficient is determined through the general formulation of the thrust force in Eq. (12).

$$C_{F,idle} = f(M, .., M^2, \delta^- 1, \sqrt{\theta}) \tag{10}$$

$$C_{F,gen} = f(C_T, .., C_T^4, M, .., M^4) \tag{11}$$

$$T = \delta \cdot m_{ref} \cdot g_0 \cdot C_T \tag{12}$$

3.3.3. Time window control system

This section introduces the control system used for the evaluation of the aircraft flight performance when required to adhere to flight schedules with TWs. The basis of the TW control system is the RTA control system available on the flight deck in aircraft equipped with a flight management system (FMS). The RTA function of the FMS has been around since the 1990's, with each manufacturer developing it's own method to calculate the required speed schedule to meet the temporal constraint. Literature exists on at least two of these methods. Smiths Industries has developed an RTA Control System that determines the appropriate cost index (CI) such that the ETA of the aircraft meets the RTA within a defined tolerance, while maintaining relative minimum fuel costs [8]. The algorithm iterates over the possible range of CI values and searches for the CI that leads to an estimated ground speed $[V_{GS}]_{EST}$ that makes the ETA at the RTA position $[t_{ETA}]_{EST}$ equal to the RTA. It assuming that the distance travelled along the flight profile is the same regardless of the CI used. This is expressed by Eq. (13), where $[t_{ETA}]_{EST}$ is flight time at the new CI, $[t_{ETA}]_{CUR}$ is the flight time at the current CI, $[V_{GS}]_{CUR}$ is the current ground speed and $[V_{GS}]_{EST}$ is the ground speed at the estimated CI. The method provided by Honeywell uses a speed adjustment parameter (SAP) to determine the speed profile to meet the RTA [15]. This parameter can be a percentage of the current airspeed, a constant airspeed adjustment or can even be the CI.

$$[t_{ETA}]_{EST} = \frac{[V_{GS}]_{CUR}}{[V_{GS}]_{EST}} \cdot [t_{ETA}]_{CUR} \tag{13}$$

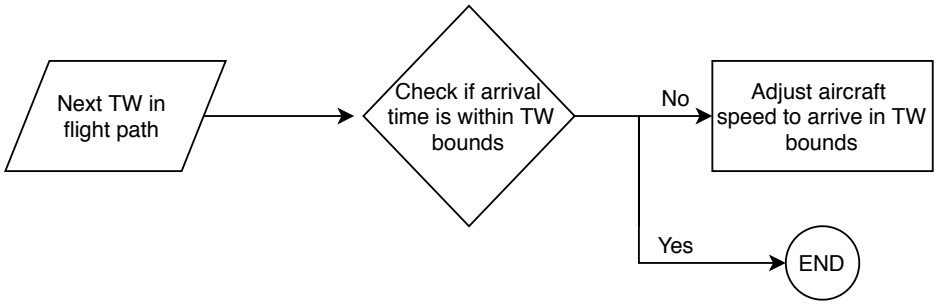

Figure 4: General overview of the TW control system logic.

Based on the two existing RTA methods, a TW control algorithm is developed to tactically evaluate the flight performance of aircraft when adhering to flight schedules with TWs. The system is modelled within the BlueSky simulation environment. Instead of iterating through a parameter to determine the required speed, the algorithm presented here iterates over the speed directly. The control algorithm has aircraft adhere to the TWs along the level-off cruise phase of the flight schedule. We consider this phase of flight as it has the largest influence on the fuel consumed. The algorithm makes use of the current aircraft flight profile (position and speed regime) to generate an ETA to the TW position. Figure 4 gives a general overview of the TW control system. For a given TW in the flight path, if the ETA is outside the TW bounds which are the opening time $t_{opening}$ and the closing time $t_{closingl}$, the control loop revises the aircraft speed until it arrives within the temporal bounds. If the required speed is outside the aircraft

flight profile the control system will try to minimize the difference between the ETA and the limiting TW bound, by flying at either the lower or upper speed limit of the flight envelope.

The sequence of functions that is performed during the TW control loop for one TW along the trajectory is illustrated in the sequential diagrams of Fig. 5. The same procedure applies for any subsequent TWs along the flight path until the end of the trajectory. The spatial and temporal position and the width of the TW are provided as input to the control system. The spatial position is defined by the latitude (φ) and longitude (λ) and the temporal position corresponds to the TW opening time $t_{opening}$ corresponding to the earliest possible arrival time at the spatial position. The latest possible arrival time at the spatial position is defined by $t_{closing}$ which is determined as $t_{opening}$ plus the TW width w.

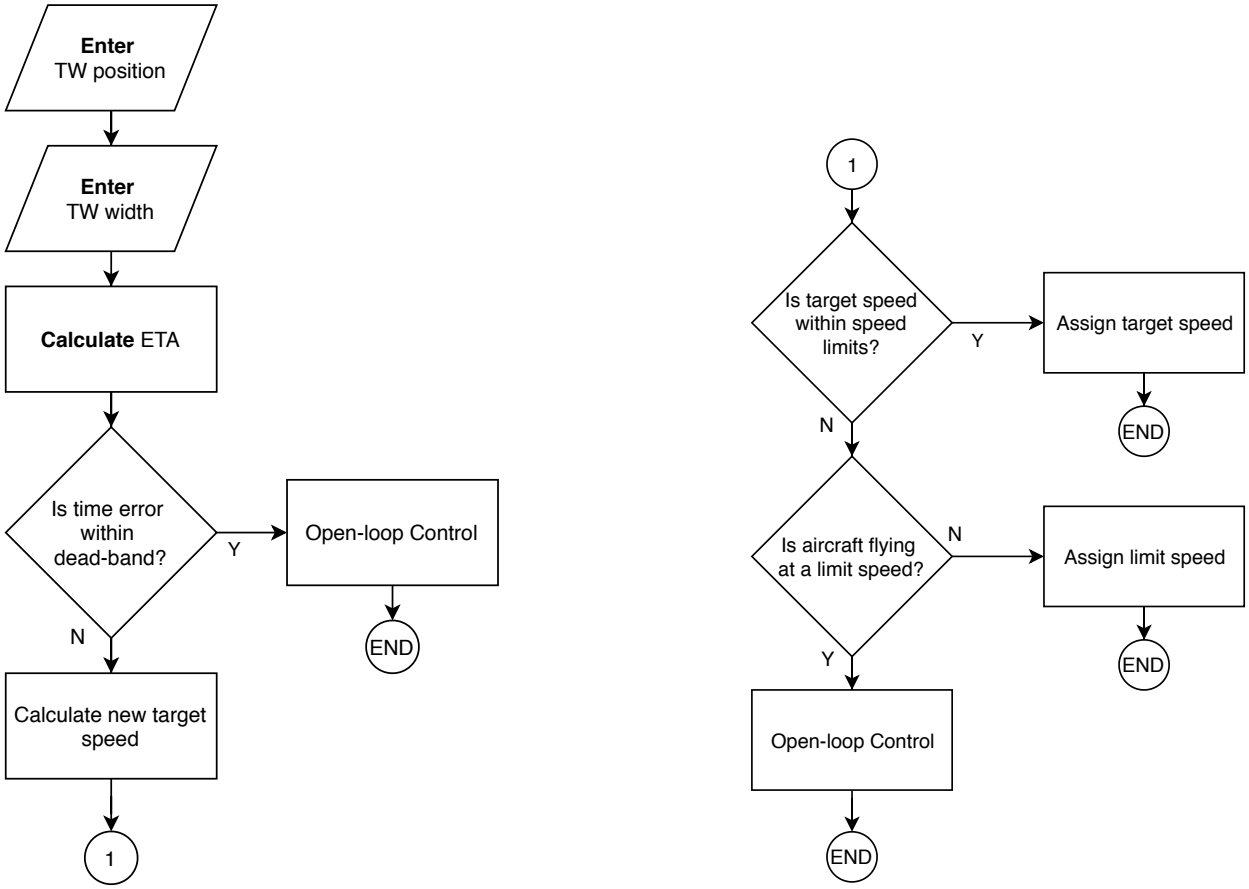

(a) Diagram showing the sequence of functions of the TW control system that determine weather the aircraft is operated in closed-loop or open-loop.

(b) Diagram showing the sequence of functions of the TW control system that ensures the aircraft is operated within the aircraft operational limits.

Figure 5: Diagram showing the sequence of functions of the TW control system.

After providing the required input, the system calculates the ETA at the TW coordinates. To generate the appropriate guidance signal to the aircraft such that the crossing time at the TW is within the time bounds, the control system must make use of a trajectory prediction. Hence, the system must determine the estimated remaining flight time on every flight segment to the TW. A flight segment refers here to the distance between two subsequent waypoints in the flight plan of the aircraft. An accurate computation of the ETA can become computationally expensive and therefore a relatively rapid estimation of the arrival time is made. Assuming there are n flight segments to the TW, Eq. (14) defines the ETA through numerical integration, where d_i is the distance between two subsequent waypoints $(\varphi_{i-1}, \lambda_{i-1})$ and (φ_i, λ_i) calculated using the World Geodetic System (WGS 84) and V_{TAS} is the current true airspeed of the aircraft.

$$[t_{ETA}]_{EST} = \sum_{i=1}^{n} \frac{d_i}{V_{TAS}} \tag{14}$$

The advantage of using the quick estimator introduces several types of errors in the TW control system. If the aircraft is accelerating or decelerating this introduces a time error in the ETA calculation, which is minor when the aircraft is relatively further away from the TW position but can become significant if the aircraft is close. Another potential type of error relates to the wind conditions used for the trajectory prediction. Wind conditions within the control system are of primary importance as they influence the accuracy of the flight profile. In conventional flight management systems, the average wind conditions between subsequent waypoints in the trajectory are used to enhance the determination of the estimated time of arrival (ETA) and to determine the speed necessary to meet a RTA [8]. This is determined based on pilot entered forecast wind data, where the information is available for every lateral and vertical waypoint. Since in the study we model the wind conditions on the day of the flight execution which the aircraft encounters along the flight path using weather forecasts, as discussed in Section 3.2.2, the ETA calculation does not explicitly take into account wind conditions. However, since trajectories are simulated using the wind spread vector and not the actual wind vector, we can assume that the average wind speeds $\bar{V}_{w,n}$ and $\bar{V}_{w,e}$ from Eq. (4) are accounted for in the ETA calculation. Following the ETA calculation, the decision to apply a guidance signal, operate in closed-loop control, or to operate in open-loop control can be made based on the time errors between the ETA and the entered $t^{opening}$ and $t^{closing}$. Therefore, two time errors are defined, one associated to each time bound of the TW. The TW opening time error $[t_{ERR}]_{opening}$ is calculated using Eq. (15) and is defined as the difference between the estimated time of arrival at the TW position and the TW opening time. Equation (16) defines the TW closing time error $[t_{ERR}]_{closing}$ as the difference between the estimated time of arrival at the TW position and the TW closing time.

$$[t_{ERR}]_{opening} = [t_{ETA}]_{EST} - t_{opening} \tag{15}$$

$$[t_{ERR}]_{closing} = [t_{ETA}]_{EST} - t_{closing} \tag{16}$$

There are two situations in which closed-loop control must be applied. The first case is when the aircraft is expected to arrive earlier than opening time of the TW, in which case $[t_{ERR}]_{opening}$ takes negative values. The second case is when the aircraft is expected to arrive later than the upper bound of the time window, in which case $[t_{ERR}]_{closing}$ takes positive values. When closed-loop control is applied, the system will try to chance the aircraft speed such that the ETA becomes equal to an input time t_{input} that is within the TW bounds. The time signal t_{input} used to determine the new target speed is given by Eq. (17). In the first case where the aircraft arrives earlier than the TW opening time, the t_{input} takes the value of the TW opening time. In the case that the aircraft arrives later than the TW closing time, the t_{input} takes the value of the TW closing time. The control system will try to adjust the aircraft speed such that the estimated time of arrival at the TW position $[t_{ETA}]_{EST}$ will be equal to t_{input}.

$$t_{input} = \begin{cases} t_{opening}, & \text{if } [t_{ERR}]_{opening} \leq 0 \\ t_{closing}, & \text{if } [t_{ERR}]_{closing} \geq 0 \end{cases} \tag{17}$$

However, the ETA cannot be made exactly equal to the $t^{opening}$ or $t^{closing}$ when a closed loop control signal needs to be applied. Therefore in order to reduce the number of closed-loop control signals created and the throttle activity, a dead band is applied to the TW bounds. The tolerance window is illustrated in Fig. 6 and includes the area above the "Active Early Control" and the area below "Active Late Control". The vertical bar indicates the TW position. The dead band configuration is dependent on the time remaining to the time window constrained way-point. For flight times larger than two hours, the dead-band is kept at plus or minus 2 minutes from the TW opening, and the TW closing time respectively. For remaining flight times lower than two hours but greater than 60 times the tolerance time $t_{tolerance}$, the dead-band is a linear function equal to 1.67% of the remaining flight time. Finally, for flight times less than 60 times the tolerance until the waypoint, the dead band is fixed at the time tolerance $t_{tolerance}$. For example, for a $t_{tolerance}$ of 6 s, when the aircraft is 60 s away from the TW position, there will be no control signal if the aircraft is expected to arrive in the time period between [$t_{opening}$ - 6 s, $t_{closing}$ + 6 s]. For the same $t_{tolerance}$, when the aircraft is

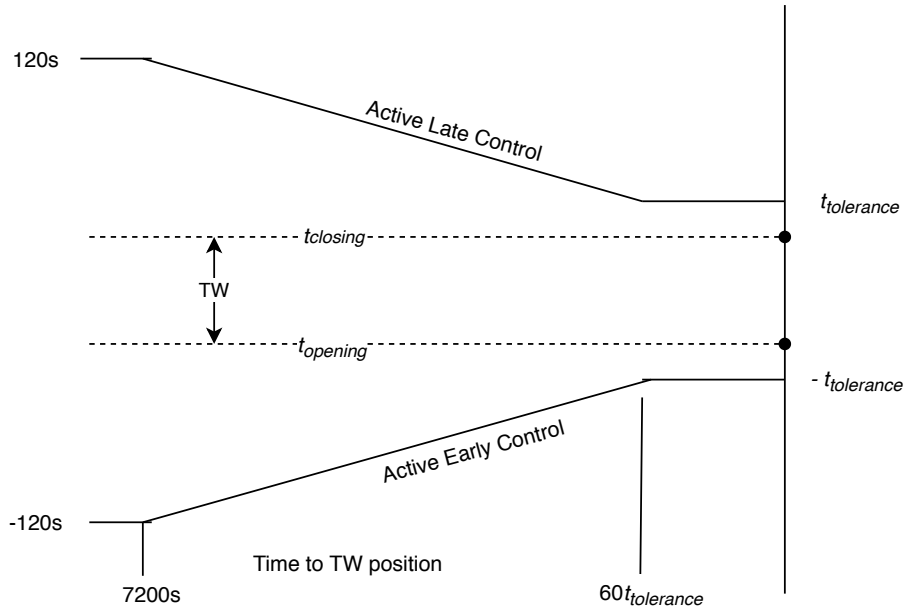

Figure 6: TW Control Loop Dead band.

3000 s, there will be no control signal if the aircraft is expected to arrive in the time period between [$t_{opening}$ - 50 s, $t_{closing}$ + 50 s].

The dead-band is adapted from that presented in [8], to determine whether the two time errors $[t_{ERR}]_{opening}$ and $[t_{ERR}]_{closing}$ are within or outside the time window. If the time errors fall within the dead band tolerance window the control system is maintained within open loop configuration. Alternatively, if either of the time errors fall outside their designated tolerance window then closed loop control is applied.

The allowable time tolerance range defined by the invention in [8] is between 6 and 30 seconds. In order to ensure flexibility in the ATC environment the pilot is required to enter the desired tolerance depending on the flight phase he is in. During this study in order to test the boundaries of the TW concept of operations a time tolerance $t_{tolerance}$ of 6 second used throughout the trajectory at all metering fixes, despite the generally large en route aircraft to aircraft spacing requirements.

Under the dead-band application, the input signal to the target speed calculation after the dead-band is defined by Eq. (18).

$$t_{input} = \begin{cases} t_{opening}, & \text{if } [t_{ERR}]_{opening} \leq -t_{tolerance} \\ t_{closing}, & \text{if } [t_{ERR}]_{closing} \geq t_{tolerance} \end{cases} \tag{18}$$

If the conditions for closed-loop operation of the TW control system are fulfilled the search for the target speed to meet the input time t_{input} begins. The method used to calculate the new speed schedule as a function of the t_{input} does not rely on the cost index or a speed adjustment parameter, but identifies directly the required speed through the equivalent range approximation. As apparent from Eq. (19), the new calibrated airspeed $V_{CAS}]_{EST}$ required to reach the time objective is defined by the ratio of the distance to the active TW and the input time.

$$[V_{CAS}]_{EST} = \frac{[V_{CAS}]_{CUR} \cdot [t_{ETA}]_{EST}}{t_{input}} \tag{19}$$

Following the determination of the target V_{CAS}/M combination, before this new speed is substituted for the current one, a check is performed as to weather or not this combination is within the flight envelope of the aircraft as is shown in Fig. 5b and defined by BADA 3.0. If the assigned V_{CAS}/M combination are within the flight envelope, they are

subsequently provided as input to the aircraft. Otherwise, if the aircraft is predicted to arrive later that the closing time of the TW and would require a target V_{CAS} or M larger than the $V_{CAS,max}$ or M_{max}, the current speed is changed to the limit speed. In the event that it is already flying at a limit speed no control signal is applied. A similar iterative process is applied if the aircraft will arrive earlier than the opening TW time and requires a V_{CAS} or M value larger smaller than $V_{CAS,min}$ or M_{min}.

3.4. Metrics

For the 20 trajectories described in Section 3.1, a simulation is carried out for each of the four TW types (1 min, strategic, pre-tactical,60 min), each of the 50 members of the ensemble weather forecast with a one day lead time and each of the five delay values(no delay, five, ten, fifteen and twenty minutes). The output of the fast-time simulations of operations is the fuel consumption over the trajectory and the arrival punctuality of the aircraft at the TWs. We define the arrival punctuality as the crossing time of the aircraft at the TW position.

The amount of fuel used during the trajectory is a function of the width of the TW. This is because the TW width determines the degree of flexibility available to execute the flight. We hypothesis that flight schedules with wide TWs along the trajectory require less speed adjustments from the optimal speed to ensure that the TW bounds are respected than narrow TWs. A higher number of speed adjustments implies more fuel burned, On the other hand, the fuel consumption is also expected to vary with the amount of delay assigned. The larger the delay the more speed adjustment are needed in order to meet the TWs and the higher the likelihood that the aircraft would have to fly closer to the maximum speed. Finally, the crossing time punctuality and the fuel consumption are influenced by the wind vector.

4. Results

The results of the fast-time simulation experiments are presented and discussed in this section in terms of the destination on-time performance (DOTP), crossing time performance (CTP) and the fuel consumption over the trajectories. In addition, the control system actions are summarized in terms of the number of guidance signals generated.

4.1. Fuel flow

The fuel flow (FF) is defined by Eq. (20) as the ratio between the fuel used during the flight time, calculated as the the difference between the initial mass m_i and the final aircraft mass m_f, and the scheduled flight time $t_{scheduled}$. The $t_{scheduled}$ is the flight duration from Fig. 3.

$$\mathrm{FF} = \frac{(m_i - m_f)}{t_{scheduled}} \ (\mathrm{kg\,s^{-1}}) \tag{20}$$

The results of the fuel flow are given in Table 3. They show the mean values of the fuel flow over the flight simulated with 50 ensemble forecast members. On average the larger the width of the TW the less fuel is required to maintain the aircraft on the assigned flight schedule. The first column of the table points to the scenario where there is no delay present. When the aircraft must adhere to 1 min TW, the fuel flow value is $0.74\,\mathrm{kg\,s^{-1}}$ which is 8% higher than when flying with flight schedules that have more flexible TWs: pre-tactical and the 60 min. The increase in the fuel flow is explained by the aircraft speed regime. From Table 4, where the percentage time that the aircraft spends at maximum speed during the flight is displayed, we can see that the aircraft ends up flying on average 33.5% of the time at maximum speed when adhering to 1 min TW with no delay. This is almost 6 and 33 percentage points higher than when adhering to the strategic and the pre-tactical schedules respectively. In addition, there are more speed changes needed to arrive within the TW when flying with a 1 min TW. Fig. 7, we can see the distribution of the speed changes, where each of the four figures corresponds to a TW type. A speed change is considered a change in the aircraft velocity of at least 1 kts. Looking at the figure corresponding to the 1 min TW in the top left corner, we observe that we almost always require one speed change to adhere to the schedule. In case there is no delay, the amount of speed changes ranges from zero to three, with three being the predominant case. This number decreases for the remaining of the TW types to zero.

The results of the simulations with departure delay are presented in the remaining columns of Table 3. If the aircraft encounters a delay the increase in fuel consumption required to compensate the delay depends on the TW

width. Typically a higher fuel consumption is observed when the delay exceeds the TW width. The peak value of $0.84\,\mathrm{kg\,s^{-1}}$ is encountered for the 1 min TW already at five minutes delay, for the strategic at fifteen minutes and for the pre-tactical at 20 minutes. We observe from Table 4 that when there is a peak value in the fuel flow, the aircraft spends 74.2% of the time at maximum speed. The maximum speed value is never reached with a 60 min TW and the fuel flow remains at more than 17% below this value. Furthermore, we observe from Table 4 that in this case the aircraft spends no time at maximum speed. In addition, the bottom right plot in Fig. 7 indicates that the aircraft was barely operated in a closed-loop control. Under 5% of flight plans require a speed change.

For each TW type, we can observe the increase in the mean fuel flow starting with simulations in which the delay duration matches the TW width. There is an 8% increase from the five minute delay simulation to the ten minute one for the strategic TW and a 10% increase from the ten minute delay simulation to the fifteen minute one for the pre-tactical TW. This simulations also exhibit a wider spread of the fuel flow. The boxplots in Fig. 8 show spread of the fuel flow for the 20 trajectories considered and their associated 50 realisations. The variability of the fuel flow increases when the aircraft encounters a delay that is equal or close to the TW width. This behaviour is exemplified by the boxplots in of the 1 min TW with no delay, that of the strategic TW with a ten minute delay and that of the pre-tactical TW with a 15 minute delay. Therefore, the spread of the fuel flow increases as a result of the TW control loop actions and effort to compensate for the delay.

Table 3: Mean fuel flow over the 1000 flight plan realisations corresponding to each simulation type.

		Delay				
		0 min	**5**min	**10** min	**15** min	**20** min
Time Window	**1** min	0.74	0.84	0.84	0.84	0.84
	strategic (TW $\leq$ 10 min**)**	0.69	0.72	0.79	0.84	0.84
	pre-tactical (TW = 15 min**)**	0.68	0.70	0.71	0.77	0.84
	60 min	0.68	0.70	0.70	0.70	0.70

Table 4: Mean percentage time flown at maximum speed over the flight plan over the 1000 flight plan realisations corresponding to each simulation type.

		Delay				
		0 min	**5**min	**10** min	**15** min	**20** min
Time Window	**1** min	33.5 %	74.2 %	74.2 %	74.2%	74.2 %
	strategic (TW $\leq$ 10 min**)**	6.2 %	14.9 %	54.9 %	74.2 %	74.2 %
	pre-tactical (TW =15 min**)**	0.0 %	0.0 %	3.8 %	50.1 %	74.2 %
	60 min	0.0 %	0.0 %	0.0 %	0.0 %	0.0 %

4.2. Destination on-time performance

The DOTP is defined by Eq. (21) as the difference between the arrival time at the last TW along the flight plan $t_{arrival,dest}$ and the scheduled flight duration $t_{scheduled}$. The $t_{scheduled}$ corresponds to the opening time of the last TW $t_{opening,dest}$ as was described in Section 2.

$$\mathrm{DOTP} \;= t_{arrival,dest} - t_{scheduled}\ (\mathrm{min}) \tag{21}$$

Table 5 presents the mean value of the DOTP over the 20 trajectories considered in the study, where each flight plan has 50 realisations obtained using the ensemble weather forecast. The first column of the table presents the values for the simulations in which the trajectories were not affected by a delay in the air traffic system. We observe that only when the aircraft must be operated using the most constraining TW type, that of 1 min, that the aircraft arrives outside the closing time of the destination TW $t_{closing,dest}$. The DOTP takes a mean value of 1.6 min, which means the aircraft arrives 36 s outside $t^1_{closing,dest}$, which is the closing time of the destination TW with a 1 min width. For the remaining three TW types, the aircraft arrives 2 min and 18 s away from $t_{scheduled}$ for the strategic TW, and just 12 s later from this value for the pre-tactical and 60 min. On average the aircraft arrives closer to the $t_{scheduled}$ of the TW and remains

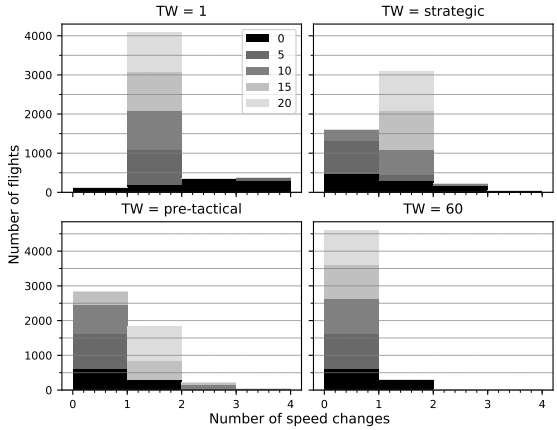

Figure 7: Distribution of the speed changes along the flight plan simulations.

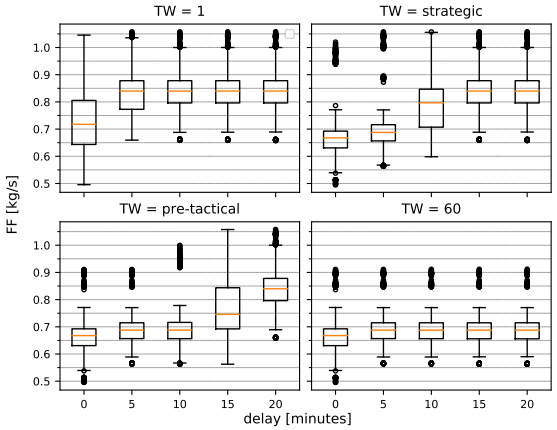

Figure 8: Spread of the FF over the 1000 flight plan realisations corresponding to each simulation type.

within the bounds of the TW. The similar result for the pre-tactical and 60 min window indicates that the flights had a similar degree of flexibility between the two types of TW during execution.

The delay in the system enlarges the DOTP value for all TW types. In the case of the extremely limited TW of 1 min, the DOTP value grows proportionally with the amount of delay. Hence with a delay of a 5 min the aircraft arrives on average 4.5 min away from the $t_{scheduled}$, which means it reaches the TW position 3 min and a half away from $t^{1}_{closing,dest}$. With every increase in delay of five minutes, the average DOTP increases by five minutes as well. The linear growth is displayed in the first row of Table 5 and is justified by the speed regime in which the control system has the aircraft fly. From Table 4, we observe that the aircraft spends 74.2% of the flight time at the maximum speed after the delay exceeds the TW width in order to compensate for the lost time when flying with the most constraining TW of 1 min.

For the strategic and pre-tactical TWs, the aircraft begin arriving outside the TW upper bound when the delay is equal to the TW width. Therefore the aircraft arrives 18 s after the closing time of the destination TW with the strategic width $t^{strategic}_{closing,dest}$, when the delay is 10 min and 30 s after the destination TW with the pre-tactical width $t^{pre-tactical}_{closing,dest}$ when the delay is 15 min. Since, the control system acts upon the aircraft in a similar manner once the delay has exceeded the TW width, we observe that the mean DOTP values are the same despite the TW type. In case of the 60 min TW the DOTP increases linearly by five minutes and because there are no speed adjustments applied as seen in Fig. 7. Therefore the aircraft maintains it's speed regime and just deviates at arrival by the delay width.

Figure 9 offers a better insight into the spread of the destination punctuality, while Table 6 shows the percentage of destination TWs in which the aircraft arrives within the TW bounds for each TW and delay type. This is also the number of DOTP values for a TW type that are smaller than the TW width. The general trend is that the wider the assigned TW the higher the percentage of DOTP values that are lower than the assigned TW. Less than half of the trajectories simulated with no delay using the 1 min TW have reached the destination TW within the bounds. This number dropping to 12% with a delay of only 5 minutes and reaching 0% with larger delays. With the strategic TWs, the number of destination TWs reached drops below 50% only when the delay reaches 10 min, while for the pre-tactical type this happens only when the delay reaches 15 min. For the remaining more flexible TW type, 60 min most destination TWs are reached, with the exception of 38. In general, the larger the TW length, the larger the delay that the aircraft can absorb en-route to arrive as scheduled.

We observe in the first two columns of Table 6, that in the case of the strategic, pre-tactical and the 60 min, the simulations with no delay results in a lower percentage of DOTP values smaller than the TW width than simulations with a delay of five minutes. As an example, for the pre-tactical TW there are 96.2% TWs which the aircraft respects, while 100% of TWs are respected with a delay of 5 min. This is due to the definition of the TWs, in which the opening time corresponds to the scheduled flight time. Therefore, with no delay the TW opening time becomes constraining.

Table 5: Mean value of DOTP over the 1000 trajectories realisations for each simulation type.

		Delay				
		0 min	**5**min	**10** min	**15** min	**20** min
Time Window	**1** min	1.6	4.5	9.5	14.5	19.5
	strategic (TW $\leq$ 10 min)	2.3	6.3	10.3	14.5	19.5
	pre-tactical (TW = 15 min)	2.5	6.7	11.5	15.5	19.5
	60 min	2.5	6.7	11.7	16.7	21.7

Table 6: Mean percentage of DOTP $\leq$ TW over the 1000 flight plan realisations corresponding to each simulation type.

		Delay				
		0 min	**5**min	**10** min	**15** min	**20** min
Time Window	**1** min	43.5 %	12.0 %	0.0 %	0.0 %	0.0 %
	strategic (TW $\leq$ 10 min)	84.1 %	84.4 %	42.4 %	10.0 %	0.0 %
	pre-tactical (TW = 15 min)	96.2 %	100 %	84.6 %	49.9 %	10.0 %
	60 min	96.2 %	100 %	100 %	100 %	100 %

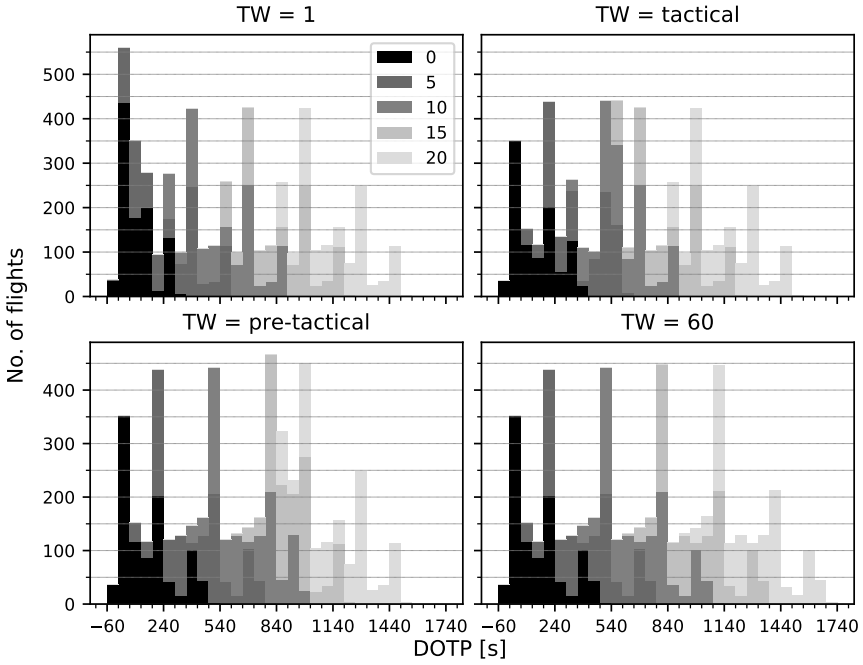

Figure 9: Distribution of the destination on-time performance over the 1000 trajectories realisations for each simulation type.

Table 7: Mean CTP over the 1000 flight plan realisations corresponding to each simulation type.

		Delay				
		0 min	**5**min	**10** min	**15** min	**20** min
Time Window	**1** min	63.8 %	5.2 %	0.0 %	0.0 %	0.0%
	strategic (TW $\leq$ 10 min)	87.4 %	85.8 %	37.1 %	2.0 %	0.0 %
	pre-tactical (TW = 15 min)	93.1 %	100.0 %	94.5 %	45.9 %	2.0 %
	60 min	93.1 %	100.0 %	100.0 %	100.0 %	100.0 %

4.3. Crossing time performance

The crossing time performance (CTP) is defined as the ratio between the number of TWs along the flight plan at whose positions the aircraft arrives within the assigned TW and the total number of TWs along the flight plan. Table 7 presents the mean crossing time performance over the 20 trajectories and their associated 50 realisations. Similar to the results in Table 6, the number of TW reached on average during each flight increases with the TW width and decreases with the delay duration. The CTP decreases below 50% when the assigned delay is close to or equal to the TW width. As an example, with the strategic TWs, the CTP values are similar with no delay as with a five minutes delay, there being less than a 2% difference between the two, but the already when the delay is 10 min the CTP drops to 37.1%. The results in the first column, which represent the scenarios in which there is no delay for any of the trajectories, indicate a good overall adherence's to the flight schedules. The highest performance is achieved with the more flexible TWs: the pre-tactical and 60 min where on average 93% of the TWs in a flight plan are respected. The biggest challenge in maintaining the aircraft on the flight schedule happens with a 1 min TW which is expected. CTP takes on average a value of 63.8% when required to adhere to flight schedules with TWs of 1 min, which means little over a half of the TWs are reached within their opening and closing time. This value drops to 5% when there is a delay of five minutes indicating that flight schedules with TWs of 1 min offer little flexibility for aircraft to operate.

5. Discussion

The purpose of this research was twofold. First, it was to introduce a speed control methodology that allows aircraft to adhere to 4D trajectories in which the time constraint is a time interval called a time window (TW). These trajectory types offer flexibility to aircraft during flight execution, while ensuring the predictability of the air traffic network since the TW widths satisfy demand and capacity imbalances. Second, a proposed control loop was used to compare the flight performance of aircraft that are required to adhere to different flexible flight schedules through simulations of operation. The comparison included flight schedules with TWs assigned in the strategic and pre-tactical planning phase as well as schedules with TW widths of 1 min and 60 min.

The fast-time simulations indicate that there is a marginal advantage for aircraft to adhere to flexible flight schedules from the perspective of their individual flight performance. The larger the width of the TWs in the flight schedule, the larger the delay that the aircraft can absorb en-route to its destination and arrive within the expect bounds of the TW. In addition, schedules with larger TW widths offer a better predictability of the air traffic system, as the crossing time at TWs along the route is more likely to be within the TW bounds even if the aircraft encounters a delay. In this situation, the aircraft also gets to keep on operating within the same speed regime as long as the delay duration is smaller than the TW width and therefore the fuel consumption does not change.

The number of flight adjustments required to maintain the aircraft on its flight schedule is inversely correlated to the TW width. However, in most scenarios the number of at least 1 kts speed changes is small or null. The maximum number of speed change requests along the trajectory is encountered with the most constraining TW of 1 min and it is three. The higher the TW width the less speed changes are needed to maintain the aircraft on the flight schedule. Furthermore, when the delay duration exceeds the TW width, there is only one speed change request for every simulation in which the velocity is increased to the maximum in order to reduce as much as possible the difference between the TW closing time and the arrival time at the TW.

The results indicate that the difference between the strategic [3] and pre-tactical [16] flight schedules is only significant in terms of the TW widths. In the case study of this paper, the pre-tactical TWs offered a higher level of flexibility than the strategic TWs, therefore they are preferred from the perspective of both aircraft and network. However, in a case where the pre-tactical TWs would offer less flexibility, in which case the widths of the pre-tactical TWs would be smaller than the strategic ones, the strategic TWs would be preferred by the aircraft. However, from the perspective of the air traffic network we would still prefer the TWs defined in the pre-tactical phase, since these take into account information from a couple of days before departure.

In addition, this study recommends further work to investigate different methods to calculate the new speed schedule when a closed-loop control signal is required and to develop control signals for all phases of flight. In this research, the method used to calculate the new speed schedule iterates directly on the V_{CAS} or Mach number by using an equivalent range formula. This method does not generate speed schedules that are "in proportion" to the original speed schedule. Most solutions in RTA control systems make use of a parameter which they iterate over to identify the

required speed schedule. In the case of the RTA system used to model the TW control system, this parameter is the CI. This information is available within the BADA 4.0 model.

Existing methods on determining the M/ V_{CAS} schedule as a function of an RTA constraint that propose an iteration directly on the M and V_{CAS} values make use of a sequence of nested intervals[7]. For example, if the aircraft is predicted to arrive later than the closing time of the TW, a new profile is calculated with a new V_{CAS} equal to half of the sum of the current V_{CAS} and the maximum V_{CAS}. Future research can make use of this method generates to generate incremental increases or decreases of the speed without using a cost index. Furthermore, future research can include all flight phases that the aircraft experiences, from departure, climb, cruise, descent and arrival. Here, due to the limitations of the chosen simulation environment BlueSky in allowing for speed commands during climb or descent, only the level-off cruise phase could be considered. However this is considered the most fuel intensive part of the flight.

6. Conclusion

This study is meant to be conductive to the introduction of strategic and pre-tactical planning though the tactical assessments of flexible flight schedules and the identification of schedules that results in a balance in adherence to the plan and fuel consumption. We have implemented our proposed model within the FMS of the BlueSky open-source simulator, which is compatible with BADA 3.0, and performed several fast-time simulations of flight schedules to determine the flight performance of individual aircraft under both departure time and weather uncertainty. The BADA 4.0 fuel consumption model was used to determine the fuel flow of each trajectory.

References

[1] T. Bolić, L. Castelli, L. Corolli, D. Rigonat, Reducing atfm delays through strategic flight planning, Transportation Research Part E: Logistics and Transportation Review 98 (2017) 42–59.

[2] P.e.a. Bougeault, The thorpex interactive grand global ensemble, Bulletin of the American Meteorological Society 91 (2010) 1059–1072.

[3] L. Castelli, L. Corolli, G. Lulli, Critical flights detected with time windows, Transportation Research Record: Journal of the Transportation Research Board 2214 (2011) 103–110.

[4] L. Castelli, P. Pellegrini, An AHP analysis of air traffic management with target windows, Journal of Air Transport Management 17 (2011) 68–73.

[5] L. Corolli, L. Castelli, G. Lulli, The air traffic flow management problem with time windows, 4th Internation (2010) 201–207.

[6] V. Dal Sasso, F. Djeumou Fomeni, G. Lulli, K.G. Zografos, Incorporating Stakeholders' priorities and preferences in 4D trajectory optimization, Transportation Research Part B: Methodological 117 (2018) 594–609.

[7] D. De Smedt, T. Pütz, Flight simulations using time control with different levels of flight guidance, AIAA/IEEE Digital Avionics Systems Conference - Proceedings (2009) 1–15.

[8] M.K. DeJonge, Required time of arrival (rta) control system, United States Patent 5121325, June 9, 1992.

[9] G. Enea, M. Porretta, A comparison of 4d-trajectory operations envisioned for nextgen and sesar, some preliminary findings, 28th International Congress of the aeronautical sciences (2012) 1–14.

[10] Eurocontrol, DDR2 Reference Manual For General Users, Technical Report, 2018.

[11] D. Gonz, M. Soler, M. Sanjurjo, Wind-Based Robust Trajectory Optimization using Meteorological Ensemble Probabilistic Forecasts, DBIAB - AERO - Proceedings 2016 (2016) 1–8.

[12] ICAO, Time adherence in TBO, Technical Report March, 2014.

[13] ICAO, Global TBO Concept, Technical Report, 2015.

[14] H. Jacco, J. Ellerbroek, BlueSky ATC Simulator Project: an Open Data and Open Source Approach, 7th International Conference on Research in Air Transportation (2016).

[15] M. Jackson, R. O'Laughlinc, E. Brian, Airborne required time of arrival control and integration with ATM, 7th AIAA Aviation Technology, Integration, and Operations Conference (2007).

[16] R.V. Mihaela Mitici, Advanced prediction models for flexible trajectory-based operations, Technical Report, ADAPT Consortium, 2019.

[17] A. Nuic, V. Mouillet, User manual for the Base of Aircraft Data (BADA) - Revision 3.6, Technical Report, European Organisation for the Safety of Air Navigation (EUROCONTROL), 2004.

[18] A. Nuic, V. Mouillet, User manual for the Base of Aircraft Data (BADA) Family 4, Technical Report, European Organisation for the Safety of Air Navigation (EUROCONTROL), 2014.

[19] D. Poles, A. Nuic, V. Mouillet, Advanced aircraft performance modeling for atm: Analysis of bada model capabilities, in: 29th Digital Avionics Systems Conference, IEEE, 2010, pp. 1.D.1–1–1.D.1–14.

[20] D. Rivas, A. Franco, A. Valenzuela, Analysis of aircraft trajectory uncertainty using Ensemble Weather Forecasts, European Conference for Aeronautics and Space Sciences (EUCASS) (2017) 1–12.

[21] R. Vazquez, D. Rivas, Chapter 4: Uncertainty, in: Complexity Science in Air Traffic Management, volume 1, Routledge, 2016, pp. 41–60.

II

Literature Study (previously graded under AE4020)

2

Trajectory-Based Operations

This chapter introduces the TBO concept, which is fundamental to the future ATM systems and defines the jargon, elements, and technologies associated with the concept. Section 2.1 outlines the role of the TBO within the European and USA modernization programmes. Secondly, Section 2.2 presents the implementation of the TBO concept of operations within the European ATM system. Due to the introduction of this concept, several changes in the flight planning methodology are expected. These changes are seen against the current practice in Section 2.3. Finally, Section 2.4 presents the key enabling technology for the introduction of TBO,the FMS.

2.1. Scope and vision

The ATM modernization programmes SESAR, and *Next Generation Air Transportation Systems* (NextGen) propose a shift in operation from the legacy paradigm of airspace-based operations to TBO. Both programmes state that the inefficiency of airspace-based operation is due to the division of airspace in fixed sectors and *Air Traffic Controller* (ATCo) workload, which limit network capacity. TBO is suppose to generate more safe and efficient use of an airspace by focusing on traffic flows instead of airspace sectors.

TBO relies on a set of enabler technologies and procedures to construct the 4DT, which is an accurate description of the aircraft path in time and space (latitude, longitude, flight level and time). As with the conventional, 3D flight planning, the procedures revolve around way-points, which are now associated with a CTAs, which aircraft must meet with a certain level of time tolerance. The agreed upon CTA constraints must be reached using on-board technology, the FMS. 4DT meet the needs of both airspace users and ANSPs as they are developed through a collaborative decision-making process involving negotiations between the ATM stakeholders.

However, there are differences in the implementation of TBO within the European and USA ATM systems. Ulfbratt and McConville [41] found that the main difference between the SESAR and NextGen TBO concepts is the focus SESAR has on the execution of the 4DT and the agreement between ATM stakeholders on the trajectory. In summary, SESAR takes a more collaborative approach, while NextGen takes a centralized approach to trajectory management with a focus on using the improved surveillance capabilities of the ATC system to allow the aircraft to fly as close as possible to its desired trajectory while ensuring network performance. This difference could be attributed to the organisational differences between governing aeronautical bodies in the USA and European states. Enea and Porretta [17] provides an example procedure in which this difference in implementation is apparent: the trajectory renegotiation process during flight. In SESAR, the assumption is that aircraft fly their filled and ANSP approved flight plans and as a result there is no need for ANSP to interfere in the aircraft trajectory. In case an aircraft has *Estimated Time of Arrival* (ETA) at a way-point that is not consistent with the CTA from the flight plan, the aircraft FMS triggers the first renegotiation, which provides ATC with the ETA as calculated by the FMS. Therefore, the aircraft limitations and environmental conditions determine the initial guess for the new CTA at the way-point. Then ATC uses information on the ATM network to derive a new CTA that is consistent with the aircraft FMS capabilities and does not conflict with the network plans. On the other hand, in the NextGen system, the assumption is that the ground system has a better overview of traffic and this will lead to a network optimal solution and hence ATC system generates the first renegotiation when it deems necessary.

The remainder of the literature reviewed for this research focuses on the European implementation of TBO. This choice was made due to the type of data available for research: flight plans and flown trajectories over European airspaxce. In the following text, all procedures and jargon refer to the specifics of the implementation as envisioned by SESAR.

2.2. TBO in SESAR

The backbone of TBO is the 4DT (also called *Business Trajectory* (BT) when referred to a trajectory in civil aviation), a 4D trajectory that is agreed upon by all ATM stakeholders, which includes airlines and ANSP. The BT, as envisioned by SESAR [38], is not static, but continuously evolves through the different planning and operation phases of a flight, through a collaborative decision-making process and shared among the stakeholders' trough *System Wide Information Management* (SWIM). The constant sharing and refinement of the BT allow all stakeholders to have the same view of the aircraft position and act on the same information. This is contrary to the current practice in which the flight plan of the ground system and that of the aircraft FMS are different.

SESAR defines two stages in the introduction of trajectory management: the *Initial 4D Trajectory Management* (I4D) and full 4D. The main reason for the two stages is that Full 4D, in which aircraft use 4DT from take-off to landing, requires complex ground infrastructure and avionics modification. SESAR has therefore proposed as a step towards full 4D, I4D. In I4D operations, the objective is to improve reliability and accuracy of sequencing arrival traffic at an airport through a designated metering fix and a CTA. The CTA is negotiated between airborne and ground trajectories, which requires far less technological improvements on both airborne and ground segment. The most crucial technologies in CTA operations are implied to be the FMS trajectory prediction capabilities as well as the controller-pilot datalink, through which sharing of trajectory occurs. This concept is expected to be implemented by 2022.

Mutuel and Neri [31] provides and overview of the first attempt to show technical and operational feasibility of the I4D in a real world conditions. Technical feasibility was assessed through a flight test that took place on 10th February 2012 which aimed to validate the concept in terms of procedures, expected tasks, HMI design and workload, and avionics interoperability, through the use of two FMS systems. The validation flight test consisted of one flight from Toulouse to Stockholm divided into six different legs each leg having a single CTA at a metering fix. Several on-board and ground systems were modified to support the I4D implementation, with the FMS being the most notable of the on-board avionics. Its performance in navigation and guidance was adapted to meet the requirements, which were set to reach the CTA with a window of 10 seconds. In terms of the on-board technology performance, all six CTA were reached within a maximum positive deviation of +4 seconds and maximum negative deviation of -1 second, according to the FMS log, while the ATC log recorded a maximum deviation of +9 seconds. Table 2.1 presents a summary of the deviation from each CTA, in seconds, for each logged data. There is a relatively small difference between the information held by the airborne and ground elements. In addition, the pilots agreed that the level of automation and communication messages between ground and air were satisfactory.

Table 2.1: Summary of CTA results.

CTA leg	**Overfly time and error**		
	FMS Log	**Crew log**	**ATC log**
1/ CTA1	+4s	+6s	+9s
2/ CTA2	-1s	+2s	+2s
3/ CTA3	0s	+1s	-2s
4/ CTA4	+2s	+3s	+1s
5/ CTA5	+1s	+1s	+1s
6/ CTA6	+1s	+2s	+3s

The focus of the trial flight was to prove the technical feasibility of the avionics and ATC system in supporting I4D and did not aim to show the operational benefits or feasibility of using the concept. A complementary test was performed in which the operational feasibility of using a CTA on a point during descent of flights coming into Stockholm, would help in delay absorption. However this did not make use of the FMS functionality of the previous test and therefore the difference between the fms-computed ETA and the ground-computed value at the metering fix and at the runway have been found to be large. Nonetheless, 92% of flights reached their CTA within a tolerance of around ±30 seconds, which, as is shown Section 2.4, is the

accepted tolerance on majority of *Required Time of Arrival* (RTA) equipped FMS.

From these results, one can conclude that the technology is there to support the I4D implementation, however the operational benefits and feasibility have yet to be validated. Therefore, further flight tests have been proposed to asses this, however as of today, none have been performed.

2.3. Flight Planning in TBO

Today, in airspaces where demand for air traffic exceeds at times the capacity ATFM is used. It is a service of the ATM system, as defined by ICAO's *Procedures for Air Navigation Services - Air Traffic Management* ICAO [26]. In Europe, the *Network Manager Operations Centre* (NMOC) of EUROCONTROL is in charge of fulfilling the function, which has been renamed *Air Traffic Flow and Capacity Management* (ATFCM) in EUROCONTROL handbooks and manuals, to emphasize the need for capacity management Tanner [40]. The process of flight planning in ATFCM begins approximately a year before the day of operation, around the time airline route and frequency planning and timetables are finalised Belobaba [2],Network Manager [32]. There are three phases to the current ATFCM:

Strategic / Long-term This phase typically begins well in advance, a year or six months before, and concludes seven days before real-time operations. In this phase, long-term demand and capacity matching are planned using *Repetitive Flight Plan* (RPL) submitted by aircraft operators. Then NMOC helps the ANSPs forecast the capacity they need to provide in each of their air traffic control centres and when and where to set regulations based on the potential imbalances due to major events (such as sport, military exercises etc.). Then the capacity commitments are fixed in a common planning document: NOP.

Pre-tactical / Mid/Short Term The phase takes place one day to six days before the day of operations. During this time, more accurate information about demand on the day of departure is available, as aircraft operators are submitting *Filed Flight Plan* (FPL) which are joined with the earlier submitted RPL. The strategic plan is adjusted accordingly to accommodate the new demand using the *Computer Assisted Slot Allocation* (CASA). From the aircraft operator perspective, the algorithm works in passive mode, as the allocation is internal to the system and is subject to change in the tactical stage. CASA uses the information about flights and regulations to assign a slot to each flight according to its *Estimated Time Over* (ETO). Each flight is given a provisional slot based on the order of its ETO in the restricted area and the reference time of the closest slot. This stage is called slot pre-allocation. NMOC publishes on D-1 this Initial Network Plan (INP) via the NOP, such that ATC units and aircraft operators are informed about the ATFCM measures that are in force in European airspace.

Tactical / Execution Finally, this phase occurs on the day of operations and consists of updating the plan with the known capacity, executing the plan and monitoring the traffic to ensure that ATFCM measures are applied. This is when slot allocation occurs, at a fixed time before the *Estimated Off-Block Time* (EOBT) of each pre-allocated flight, the slot is allocated to the flight and the aircraft operator and ATC are informed. In this phase, tactical measures, such as traffic re-routing and slot re-allocation, are also applied in case of delays. Moreover, the slot allocated to a flight may be improved by the true revision process.

The NMOC receives all FPL between three and 120 hours (five days) before the requested EOBT. Given the fact that the time window for airlines to file flight plans is close to the EOBT, flight dispatchers in an airline *Operation Control Centre* (OCC) have a lot of time to determine the optimal flight plan for their operations, since they have available ongoing airline operational information and forecast weather conditions. This gives an airline the advantage in flight planning as they can create the most convenient plan for them without having to take into account nominal airspace capacity or constraints of other operators. However, this does not lead to the optimal solution for the ATM network as the available capacity is planned for months in advance and only incremental adjustments can be made as the day of operations approaches.

From the above description it also becomes apparent that flight planning also only takes into account one particular ATM service, demand and capacity balancing. The current paradigm of airspace-based operations does not and cannot consider strategic or pre-tactical conflict management given the amount of information that would be needed in advance to perform such a service. In order to deliver this service, the system relies heavily on ATC interventions during flight execution. Therefore, constraints from other ATM functions are either planned last minute since the demand for air travel is known on the day of operations or satisfied during flight execution. As a result, the predictability and efficiency of aircraft trajectories is limited. The BT

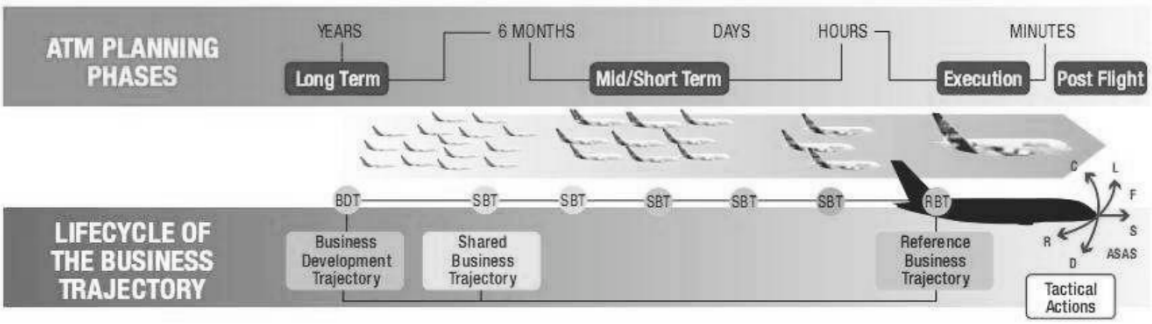

Figure 2.1: Lifecycle of the business trajectory. [42]

of TBO is suppose to enhance the predictability of aircraft trajectories and efficiency of flights, by reducing potential conflicts and demand-capacity balancing through planning. At the different ATM planning phases, the BT exists in a different state, as is shown in Fig. 2.1. The states of the BT, as defined by SESAR Consortium [39], are:

***Business Development Trajectory* (BDT)** can be planned in the strategic phase, depending on the needs of the specific airspace user operation. Typically the trajectory is not very detailed but is required to develop airline schedules. It does not get shared outside the organization. Internally it goes through several iterations to match arising constraints.

***Shared Business Trajectory* (SBT)** is the version of the BDT that the airline considers sufficiently mature to get published and that reflects their operational needs and some business constraints. It is used to carry out ATFCM planning actions. Typically this starts six months from the day of operations. The SBTs need to match network constraints. If conflicts occur, the airline is asked by ANSPs to reevaluate the trajectory. This process can take several iterations, which is what makes the BT different from the current practice in ATFCM. The benefit of the SBT is the fact that it facilitates the creation of strategic and pre-tactical network plans that include tactical information, such as meteorological data or en-route constraints.

***Reference Business Trajectory* (RBT)**. The planning ends once the RBT gets published, which occurs hours before the operation. It is the reference used by all ATM stakeholders during the flight execution. Note, the RBT itself does not represent a clearance, but a goal which is progressively authorized. The ATC clears successive RBT. Constraints to change the RBT can arise from both ground and air so that the trajectory is progressively updated and shared. Its the fact that it is continuously shared and managed among ATM stakeholders, that allows the RBT to increase predictability in the ATM system while maintaining safety. As mention in Section 2.1, the aircraft FMS computes and shares with other stakeholders the RBT.

2.4. Enabling technologies

In order to achieve TBO, there are several key enabling technologies that must be implimented either in the airborne or ground segment. Enea and Porretta [17] lists the most notable as being:

fms Modern day avionics are capable of meeting a CTA with 4 seconds accuracy, however they must be capable to support the 4DT negotiation process as well.

Data communication The current voice communication between the cockpit and ground will not be able to support 4DT operations and therefore a digital communication must be added. This could be introduced through the existing ACARS.

ADS-B The technology will be used both on the ground (ADS- B out) for surveillance and on board of the aircraft (ADS-B in) for augmented traffic situational awareness.

The capabilities of modern FMS make it an instrumental component within the trajectory-based traffic management concept. It is expected to support trajectory negotiations, through enhancements in its trajectory prediction abilities and the digital data-link communication, as well as meet the requirements on 4D navigation precision. Although FMS that support I4D management have been developed and are expected to

be implemented in more than 250 aircraft by 2022, there is limited literature available on what modifications the FMS is going to suffer to meet the Full 4D concept.

The current FMS technology reduces crew workload by automating several in-flight functions such as navigation, flight planning, trajectory prediction, performance calculations, and guidance Walter [44]. It allows, the flight dispatchers to upload the operational flight plan, several hours before the flight departure, which is then delivered pre-departure, along with up-to-date wind and temperature information, to the fms via a digital message system ACARS or company lines. Besides, pilots can also adjust the flight plan throughout the flight, based on clearances from ATC or updated information from OCC, since the current flight plans are not binding. Using the flight plan and navigation computations, the fms calculates the 4D flight profile for each phase of flight based on the performance mode of operation selected by the crew and commands are generated that keep the aircraft along both the lateral (LNAV), and the vertical (VNAV) planned trajectory profile. In the current environment, the FMS performance modes depend on direct company policy. The cruise modes are: Walter [44], Roberson [37], Customer Services AIRBUS [13]:

Fixed airspeed In this mode the aircraft operates at a specific altitude with a fixed airspeed. The associated ground speed is different since it depends on wind conditions.

Minimum trip time This mode provides the speed at which the aircraft has to fly to achieve a given mileage in the shortest amount of time. This mode is the same as maximum *Cost Index* (CI).

Maximum Range Cruise This mode allows the aircraft to achieve the best fuel mileage. Same as CI = 0.

Economy (ECON) This mode of operation keep the aircraft at the speed that results in minimum operating cost, based on the CI and the prevailing wind conditions. The airline CI is the ratio of time-related cost (typically includes maintenance, flight crew, depreciation and leasing of aircraft) and fuel-related cost of operation of a flight, as can be seen from Eq. (2.1).

$$CI = \frac{\text{Time cost}}{\text{Fuel cost}} \tag{2.1}$$

The cost index allows airlines to perform a trade-off between fuel burn and trip time. When fuel-related costs are large, the CI has a value of 0, which leads to minimum fuel consumption for maximum range. In this case, the ECON speed equals maximum range cruise speed. When time-related costs have the greatest influence on operating costs, the CI takes its maximum value, which allows for minimum trip time for maximum speed. Airlines typically have a default company CI. However, the CI used on an individual flight may be different from the company CI for many reasons: the flight experiences a delay, the route used.

Required Time of Arrival RTA This mode uses a speed that minimizes the operating cost while ensuring that the aircraft reaches a way-point at a given point in time, for the given wind conditions. The RTA function tries to eliminate the difference between ETA and the RTA by either a speed up or speed down command that is within the limits of the aircraft performance. The ETA is computed using the on-board trajectory prediction model and a wind profile which is relatively coarse. Typically, the FMS allows pilots to enter wind data of three to five different flight levels and on ground which is linearly interpolated to obtain the wind profile. In order to minimise the throttle activity, the RTA function is triggered only when the difference between ETA and RTA is above a certain tolerance. This tolerance is dependent on the avionic manufacturer and on the phase of flight the aircraft is in.

De Smedt and Berz [15] presents the availability characteristics and performance of the RTA function on modern day FMS systems of short-to-mid range aircraft (A320 and B737) in a terminal airspace context. In terms of availability the authors found the numbers from Table 2.2 on RTA equipped *Instrument Flight Rules* (IFR) flights in Europe.

Table 2.2: RTA Equipped Flights in Europe.

Specified RTA Tolerance	**GPS time**	**Flight Phase**	**Flights in Europe [%]**
±30 sec	No	Cruise	40
±30 sec	Yes	Cruise	28
±6 sec	No	Climb,cruise,descent	21
±6 sec	Yes	Climb,cruise,descent	11

The performance of the RTA function in a terminal airspace context with one RTA fix was assessed using A320 and B737 flight simulators. The authors conclude that the RTA tolerance of ±6 or ±30 seconds

is achievable under a set of pre-described conditions. The authors conclude the following about the performance and specification of the function:

- The range of permissible inaccuracies in wind and temperature predictions, and the operating envelope should be provided when manufacturers provide a tolerance value between RTA and ETA.
- The ETA update rate impacts the target speed to meet the RTA which results in time errors.
- To ensure spacing in a terminal airspace using RTA constraints, FMS algorithms would need to be robust enough to consistently achieve arrival times within less than the current state of the art of ±6 seconds (11%).

3

Time adherence in TBO

The core of TBO is the 4D trajectory which is based on the integration of time within the existing three spatial trajectory. Any delay will cause a distortion of the trajectory and therefore, a crucial element in the implementation of TBO becomes the way the time constraint over a point in the flight path is defined. These time constraints may specify an absolute value or a range. This chapter takes a look at the existing literature that discusses a range formulation for the time constraints in TBO. First, the benefits and drawbacks of using a range formulation are outlined in Section 3.1. A brief overview of the existing literature is provided in Section 3.2. Next Section 3.3 presents several studies that tackle the operational feasibility of trajectory constraints, with a special focus on time constraints. However, these earlier studies lack the mathematical formulation that would allow for ATFCM optimisation at a European network. Finally, Section 3.4 outlines the existing algorithms that focus on satisfying ATFM network constraints though the use of time fix, while Section 3.5 focus on mathematical models that make use of time windows.

3.1. Flexibility versus predictability in TBO

The primary role of the ATM modernisation programmes is to enable the safe and expeditious handling of air traffic, while not adversely affecting the aircraft operator's optimised trajectories to the extent possible. The stakeholders that stand to benefit the most from the introduction 4D trajectories are the ATC and airports, since this will increase the predictability of the aircraft position. Airlines on the other hand will have less flexibility in flight planning, since they have limited influence on the flight plan in the short-term decision-making phase. Given the inherent uncertainty associated to their operations, in the future this could leave airlines with less efficient operation compared to today, since less up-to-date information such as: schedule changes, maintenance, ground crew activities, turnaround etc. will be included in the flight plan of an aircraft. In addition, Castell [7] found that SESAR does not consider the current OCC responsibilities of short-term operational planning which aims to minimise unforeseen cost, cancellations and delays.

Therefore, the development and the implementation of the TBO concept requires the development of models and algorithms that will allow trade-offs between the user and the system optimum trajectories. International Civil Aviation Organisation [27] recognises the importance of achieving the balance between the different trajectory constraints. They hypothesises that predictability and flexibility do not generate conflicting requirements, if tolerance levels are introduced before the RBT is published. They outline a method of introducing tolerance in the RBT, by defining a range around the controlled time in which the aircraft must arrive at a metering fix. This time interval is refereed to in literature as TW.

3.2. Literature overview

The first major distinction between literature on time adherence in TBO can be made based on the trajectory constraint that the aircraft must meet. The *International Civil Aviation Organisation* (ICAO) [1] defines a trajectory constraint as a limit in the freedom of a trajectory through a limit on a 4D point or segment in one or more dimensions: lateral,vertical or time. Based on this definition of a trajectory constraint, there are two distinct categories of literature that deal with time constraints: ones that deal simultaneously with both

[1] https://www.icao.int/airnavigation/tbo/PublishingImages/Pages/Why-Global-TBO-Concept/

spatial and temporal constraint and ones that deal with just a time constraint. A further distinction can be made between literature that focuses on a temporal fix and those that focus on a time interval.

The second distinction in literature can be made based on the ATM flight planning phase for which the models were developed. The planning phases are listed in Section 2.3. Finally, the last feasible categories are the author's proposed method of computing the time constraints and the type of network constraint, either *Demand and Capacity Balancing* (DCB) or conflict avoidance that the method, that the model targets to satisfy.

In Table 3.1 the division of all the relevant papers into the categories mentioned above is made. In the following two sections the models are discussed individually.

Table 3.1: An overview of the time adherence literature

Trajectory Constraint	**Planning phase**	**Publication**	**Method**	**Network constraint**
Spatial and temporal interval	Strategic, Pre-Tactical, Tactical	Berechet et al. [3]	Reachability simulations based on aircraft performance model.	Conflict avoidance and DCB
	Tactical	Margellos and Lygeros [29]	Reachability simulations based on aircraft performance model and Monte-Carlo simulations.	Conflict avoidance
	Strategic	Gatsinzi et al. [20]	Integer Linear Programming (ILP)	Conflict avoidance
	Pre-Tactical	Dal Sasso et al. [14]	ILP	DCB
Temporal fix	Tactical	Bertmimas and Stock Patterson [4]	ILP	DCB
	Tactical	Bertsimas et al. [5]	ILP	DCB
	Strategic	Bolić et al. [6]	ILP	DCB
Temporal interval	Strategic	Corolli et al. [11]	MILP	DCB
	Strategic	Castelli et al. [9]	ILP	DCB

3.3. Spatial and temporal intervals

Early research focused on the development of trajectory constraints that had both a target time interval and target lateral and vertical interval. These 4D spatial-temporal constraints are known as target windows. Their goal was to manage uncertainty in flight operations through the sizes and locations of the target windows.

The notion of target windows was introduced in Berechet et al. [3], as an addition in the implementation of BT that would provide a balance in predictability and flexibility in TBO. They propose that these target windows be computed at every stage within the life-cycle of the BT, described in Section 2.3. The target windows would be published and negotiated at the same time as the RBT and negotiated throughout the flight duration in case conflicting constraints from stakeholders arise. The life-cycle of the target windows, alongside that of the BT, is shown in Fig. 3.1. Given their inclusion in the BT planning, the target windows are expected to facilitate air traffic management. In this paper, the target windows are defined at the transfer of responsibility area between two ANSPs, which can either be a vertical or a lateral border between sectors.

The general methodology proposed to calculate the target windows involves fours steps. This is a trajectory central methodology, where the focus is on developing a target window for each aircraft and then deconflicting them. It is important to outline that this method of computing the target windows assumes that the time of departure/arrival at origin/destination is fixed by DCB measures and is known. Therefore, the target window generation happens in each ATM flight planning only after the slot pre-allocation/ allocation. The steps are as follows:

Quantifying the uncertainty at a crossing point The crossing point is where the aircraft 4D trajectory meets the transfer of responsibility area. These crossing points are determined using aircraft performance (*Base of Aircraft Data* (BADA)) and airspace topology data through a trajectory prediction. The uncer-

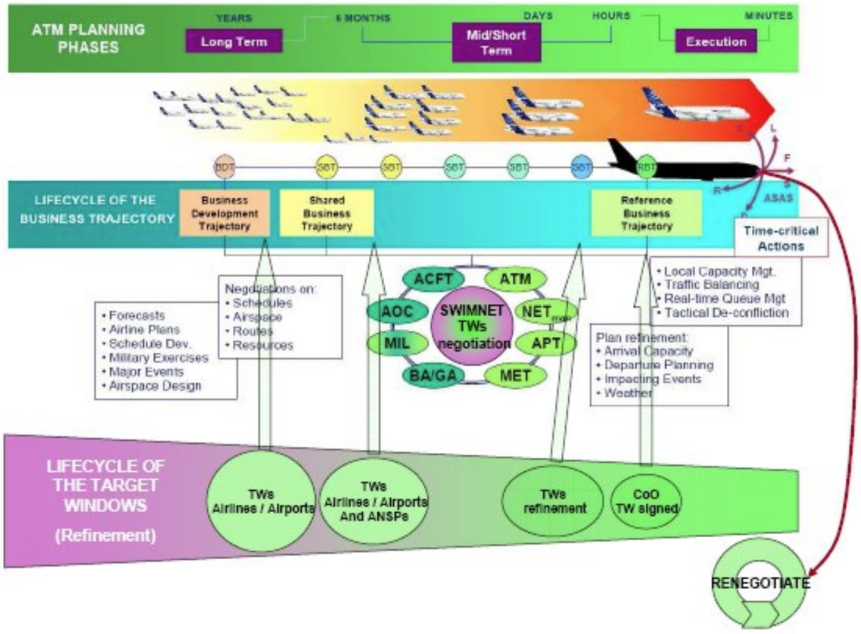

Figure 3.1: Target window lifecycle. [24]

tainty at the crossing point is modelled as directly proportional to the distance between the crossing point itself and the departure airport. It is also a function of the specific Origin/Destination pair, of the Flight Level and specific time on the point.

Determining allowable positions based on tolerances. Since the aircraft must reach the destination airport within a certain time tolerance, the aircraft must stick to a set of combinations of spatial and temporal points that allow it to meet such tolerances. The number of available points increase with distance from the destination airport and are also a function of specific destination airport, the Flight Level and the flight envelope (minimum and maximum speed)

Integration of individual specific constraints. These arise as a result of, but are not limited to, airspace boundaries, target window negotiation processes, direction of flight etc.

Final refinement of all target windows in the system. De-conflicting any possible target windows through time separation, vertical separation, horizontal separation or a combined time-vertical- lateral.

An operational assessment of the concept was performed as to asses the impact it would have on ATC and pilots' working methods. This assessment consists of a *Human-in-Loop* (HIL) experiment, a real-time simulation on the airspace composed of two en-route sectors at the border of two European Area Control Centre's (Milan and Geneva). The following three simulation were performed to asses the impact on the workload of:

- ATCo in the airborne cycle
- ATCo and aircrew in the airborne cycle
- Airports, airlines and ANSP during the renegotiation process.

In the first two types of experiments the target windows would not be altered during the flight execution. Due to the novelty of the target window concept, there is no operational information on the relation between aircraft position uncertainty or tolerances and origin-destination pair or flight level or time on point. Therefore, the first two steps in the target window generator were based on a model especially developed for the experiments by Air France Consulting. The uncertainty and tolerance are no longer dependent on the unavailable data listed above, but just on the distance of the aircraft from the departure/arrival airport. For each flight the minimal value of uncertainty is at the departure airport and its maximum level at a certain point determined by the experts. On the other hand, the minimal value of tolerance is at the arrival airport and the maximum at the point of maximum uncertainty. The possible aircraft position uncertainty and tolerance are then determined as a linear interpolation between the minimum and maximum values. The uncertainty

and tolerance cones, overlap at the maximum level of uncertainty point, and create a tube of manoeuvrability freedom. Since the minimum and maximum values are based on expert opinion and are determined per flight, where a large number of flights (>80) were considered in the airspace sector, they were not presented within the paper. As a result of this new method of computing there were three different transfer of responsibility areas considered with respect to the maximum uncertainty point: an area before, directly including the uncertainty point and an area after.

In total, the three types of experiments previously listed combined with the three possibilities of area placement resulted in nine separate simulation trials, for which 1284 target windows were constructed and assigned to 616 flights. Statistical data on the 4D dimensions of the time window shows that:

- 50% of target windows were distributed between 4'52" and 5'44".
- 50% of the target windows had a spatial width narrower than 7 NM, with the lower bound of 4 NM and an upper bound of 18 NM (reached only in 2 cases).
- 75% of target windows had a flight level window consisting of 3 admissible levels (this is due to the fact that aircraft are required to adopt flight levels according to their direction.

The paper of Berechet et al. [3] focuses on describing the target window generation algorithm. The results of the nine simulation experiments are summarised by Guibert et al. [23],Guibert et al. [24] and Guibert and Guichard [22]. In HIL-1 and HIL-2, two independent variables were manipulated: the traffic load and the target windows. The traffic load was set to either the 2008 traffic level and the 2020 forecast traffic, while the target windows were either present or absent. In the case of HIL-3, in which the impact of the renegotiation process was considered, the second independent variables was no longer the target window, but the presence or absence of the renegotiation. Two measurements were assessed during the experiments: the overall system performance and human impact. In Table 3.2 presents the indicator and associated metrics for system performance, build using various techniques, such as observations, recorded data, questionnaires and self-assessment. On the other hand human impact was measured through ATCo workload, situational awareness, usability and acceptability in HIL-1, while in the remaining two experiments the collaboration between stakeholders was also considered.

Table 3.2: Metrics used to evaluate the system performance in the CoO validation experiments.

Performance Indicator	**Metrics**
Safety	Potential losses of separation Aircraft separations
Efficiency	Number of fulfilled target windows Number of renegotiated Target windows planned flight time divided by flight time into the sector Aircraft fuel consumption Time needed to renegotiate target windows.
Capacity	Number of aircraft crossing the sector each hour Instantaneous number of aircraft ATCO instruction number (speed, heading, flight level)
Predictability	Planned flight time divided by flight time into the sector Number of fulfilled target windows

All participants were very positive about the possible implementation of the target window. Table 3.3 shows the main findings for each human impact indicator. It was shown that the target window management and the renegotiation process did not exceed human limits for any of the actors involved, although the implementation of some of the enabling technologies mentioned in Section 2.4 would help with target window management. In addition, all actors involved in the experiment found that the stakeholder that would benefit the most from implementing CoO would be the airline.

In terms of system performance, the metrics used for each indicator were consistent trough out the three experiments. The following are a summary of the system performance findings: the author concluded that the target window did not impair traffic predictability, and may even improve it with an appropriate control sector shape, size and airspace structure. By keeping the traffic level as an independent variable, the author showed implicitly that the 2020 expected capacity can be properly and safely managed. Efficiency was shown through the flight duration in a sector and the number of fulfilled time windows. The flight duration is closer

Table 3.3: Summary of human impact measurements in the HIL experiments conducted for CoO.

	Indicator	**HIL 1**	**HIL 2**	**HIL 3**
Human Impact	Workload	Statistically, the workload was not impacted by target window management, although controllers perceived it as an additional task.	Statistically, the workload was not impacted by target window management, although controllers perceived it as an additional task. The pilot workload was significantly increased by the target window management, which they found crucial in abnormal operations.	Controller workload was not impacted by renegotiation, with only the duration or change in flight level playing a role in their workload. However, pilots felt that their workload was highly increased during renegotiation but it could be improved by the use of a digital datalink.
	Situational Awareness	Statistically, traffic load of 2020 impacted more the situational awareness of controllers than target window management. Controllers felt that the target windows increased their situational awareness.	Controllers felt that target window information increases the traffic picture, although statistically there is no proof. For pilots, there is no significant difference between the 'without target window' and 'with Target window' conditions.	Neither controller or pilot situational awareness was impaired by the renegotiation process.
	Usability and acceptability	Controllers found target window management easy to learn and to use.	Pilots also found that target window management is easy to learn and to use. They feel though that target windows management requires more communications between the captain and the first officer.	Pilots found that the renegotiation process was not properly supported by the onboard equipment.
	Collaboration	-	Both stakeholders found that there is no need for an increase in communication, just for the appropriate phraseology and that the target windows should be included in the flight plan.	Communication between ATCo depends on the number of renegotiations and their associated severity. The higher they both are the higher the chances the collaboration work becomes appreciable. Communication between ATCo pilots were not affected, but can be facilitated by a digital datalink.

to the planned flight plan with target windows than the scenario without at both capacity levels. 4% of target windows were not fulfilled at a 2020 traffic level, whereas all were fulfilled in a 2008 scenario. In addition it was discovered that this is sensitivity of the fulfilment rate to airspace shape. There is no significant differences between the "without target windows" and "with target windows" conditions, whatever the level of traffic load and the measured sector and the controllers successfully separated the aircraft whatever the experimental conditions.

The study by Castelli and Pellegrini [8] compares the implementation of the BT with target windows and the current airspace-based operations to prove that implementing the former of the two concepts is beneficial for all major ATM stakeholders: airline, airport and ANSP. They looked both into the execution and planning phase. The potential benefits and limitations of the target windows are identified using *Analytical Hierarchy Process* (AHP) models, which are typically used in group decision making. There are six hierarchies constructed one for the planning and one for the execution phase of flight for each of the three stakeholders. From each hierarchy, the stakeholder can choose their maximum utility, defined by the difference between benefits an drawbacks. The experts found that the airline and ANSP benefit from the introduction of the concept in both planning and execution phase while the airport representatives place more importance on the optimization of current resources than on the benefits added by the concept. The authors attribute this shift in priority of the third stakeholder to the economic situation in which the research was conducted, namely the post 2008 economic crisis.

Margellos and Lygeros [28] aimed to quantify the freedom that target window constraints provide to aircraft compared to a metering fix though reachability methods and computational tools based on game theory. They propose a mathematical model to calculate the manoeuvrability tube the aircraft must adhere to in order to meet the target window from Berechet et al. [3]. Given the fact that it is based on reachability methods, which make use of a state space representation of the aircraft dynamics, the model is designed using an aircraft performance model and focuses again on the development of a target window for one aircraft, without taking into consideration the network picture. The target window size is not defined through the methodology, but extracted from the HIL experiments conducted within the CoO project previously mentioned. Then, the authors applied backward reachability, to calculate from a target window, which represents the final state of the state-space system, the set of 4D initial states from which the trajectories can reach the terminal states. This leads to a tube of possible positions that an aircraft has to be in within a fixed time horizon. They use a simplified two-state model to capture the aircraft dynamics based on which the reachability problem is formulated as a pursuit-evasion game.

Conflict avoidance is an essential ATM function that ensures airspace safety. In the current flight planning context, where flight plans only get shared a few hours before operations, conflicts only get resolved at tactical level through speed constraints and vertical or lateral path extensions. This approach does not guarantee an efficient solution for the ATM network, since early resolution manoeuvres may impact the time schedule of the aircraft. The TBO concept is expected, through the early information sharing. Margellos and Lygeros [29] extended their previous research on the target window and reachable tubes to construct conflict-free tubes based on an reach-avoid computation. First, using a similar methodology to Margellos and Lygeros [28], the aircraft manoeuvrability tube is constructed, which consists of start states that allow the aircraft to meet its target window along the trajectory. The algorithm was applied on a set of 50 trajectories, using 117 target windows, extracted from the HIL-2 experiment. Therefore, the position of the target windows is not optimised. The hitting probability of a target window was evaluated via Monte Carlo simulations, in which uncertainty in wind, aircraft mass, entry time uncertainty and nominal speed uncertainty. Then conflict probability was evaluated on pairs of flights most likely to be in conflict using also Monte Carlo simulations. The limitation here is that only pairwise conflict were solved without considering the possibility that the resolution command causes subsequent conflict.

Literature on mathematical models for deriving target windows at a strategic or pre-tactical network level to satisfy demand and capacity imbalances is limited to a recent study by Dal Sasso et al. [14]. The model is build for the pre-tactical flight planning of 4D trajectories, and incorporates stakeholder preferences through a tri-objective function. It minimises the total time deviation from the scheduled time of operations in the strategic phase, the cost of the flights deviating from their preferred 3D-routes and the total ANSP route charges for each flight.

The model makes use of an arc formulation: arcs connect all nodes in a network, which can be either airports or way-points. The arc can be entered by an aircraft at any flight level. A flight goes through a sequence of way-points from the departure to arrival, and each of these way-points belongs to an airspace sector. Therefore the model is a 4D-trajectory based since it considers the arc being flown in the 2D-space,

the specific altitude of the flight as well as the time periods. Eq. (3.1) defines the decision variable of the model.

$$x^{f}_{e,l} = \begin{cases} 1 & \text{, if flight } f \text{ is planned to enter arc } e \text{ at flight level } l \text{ by time period } t \\ 0 & \text{, otherwise} \end{cases} \tag{3.1}$$

The computational experiment in which the model is analysed consists of 10 test of various size and characteristics. The main parameters that define the size of each of the test are: the number of flights, the number of flight levels, the number of airspace sectors, the number of way-points, the number of airports and the democratisation of the time horizon. The parameters were constructed synthetically in the pre-processing phase. In terms of the effectiveness of solving the model, the authors found that the computational time for each non-dominated solution varies with the structure of the network. It takes approximately 3h to calculate approximately 70 non-dominant solutions for the scenario of 10,000 flights. However, since in practice only one would be implemented the computational time could be manageable.

3.4. Temporal fix

The other type of trajectory constraints that the aircraft can meet in TBO operations are constraints that involve only the temporal element. These, as can be seen in Table 3.1, can be either a fix or a time interval. The development of such constraints is typically connected to the construction of a network schedule which serves to satisfy the ATFCM function. The scope of ATFCM within the European ATM system was treated in Section 2.3. Time constraints in strategic or pre-tactical network plans are a solution to reduce ATFM delay by increasing predictability of aircraft trajectories. This is consistent with the TBO concept of operations.

Time constraints were first introduced in the mathematical formulation of the ATFM model of Odoni [35]. Developed for the tactical planning phase, the model attempts to prevent local demand-capacity imbalances by adjusting the flows of aircraft trough ground holdings. This early model did not explicitly aim to assign an arrival time or time interval at a way-point/sector entry point, but rather determined a time period in which an aircraft must depart from an airport that would minimise the cost of delay in the network. The binary *Mixed Integer Linear Programming* (ILP) model has one decision variable which takes the value of 1, when a flight f arrives at sector j by time period t and 0 otherwise. Eq. (3.2) defines the decision variable. The ATFM makes use of airline filed flight plans to set the time constraints and although established in the context of airspace-based operations, the model requires no major modification to support trajectory-based operations at a strategic planning phase. Implementing the ATFM at a strategic level requires using SBT as input to the model and using the solution to facilitate negotiations between airspace users and ANSP.

$$w^{j}_{f,t} = \begin{cases} 1 & \text{, if flight } f \text{ arrives at sector } j \text{ by time period } t \\ 0 & \text{, otherwise} \end{cases} \tag{3.2}$$

The initial study only considered *Ground Holding Delay* (GH), since the addition of fuel and safety costs associated to *Airborne Holding Delay* (AH) would not be beneficial. However, in the European ATM system, en-route traffic congestion is one of the main reasons for flight delays and ATFM strategies that considered AH were considered. AH requires speed adjustment of aircraft while airborne taking into account airspace capacity. The model proposed by Bertmimas and Stock Patterson [4] is an variation of the ILP of the Odoni [35], in which the objective function minimises a weighted sum of the cost of GH and AH. This model calculates the both the optimal departure time and sector occupancy for each aircraft based on both airport and airspace capacity. The authors also showed how the model can be extended to include rerouting as an additional option to manage delay. This could be achieved through either a path formulation or a sector formulation. The former of the two had to have the decision variables redefined to Eq. (3.3), while the latter to Eq. (3.4)

$$w^{jr}_{f,t} = \begin{cases} 1 & \text{, if flight } f \text{ arrives at sector } j \text{ by time period } t \text{ along route } r \\ 0 & \text{, otherwise} \end{cases} \tag{3.3}$$

$$w^{j'j}_{f,t} = \begin{cases} 1 & \text{, if flight } f \text{ arrives at sector } j' \text{ from sector } j \text{ by time period } t \\ 0 & \text{, otherwise} \end{cases} \tag{3.4}$$

The advantage of a recent model by Bertsimas et al. [5] is that it overcomes some major limitations of the previous ATFM models: the scale of the problems and the range of decisions to manage delay. The scale

of the problems that the model can tackle is comparable to the two largest ATM systems in the world: the USA and Central European. This model simultaneously deals with airport and en-route congestion through a large range of available decisions: ground holding, airborne holding, flight rerouting and speed control.

In this model, the airspace is subdivided into sectors of equal dimensions that form a grid. An origin-destination route is made up of a collection of subsequent sectors. The route is modelled as a directed graph in which the nodes are either sectors or airports and an arc exists between two nodes exists if sectors or airports are contiguous. A flight cannot move from a node unless the minimum number of time periods to transverse that sector has elapsed. This implicitly also determines the maximum speed between two sectors. The width of a time period and the minimum time to transverse a sector is set equal for all flights and all sectors. This limits the generality of the results since in reality the time it takes to transverse a sector is directly proportional to the sector size and sectors in ATM systems are not equal in dimensions, especially in the European system. In addition, the authors do not mention the physical size of a time period.

Capacity here is modelled as the number of aircraft in a sector in a given period of time t or the number of aircraft that can depart or arrive at an airport in time period t. In the experiments congestion is simulated by reducing the capacity in some sectors from the nominal capacity. The authors mention that the nominal capacity allows for serving aircraft without incurring serious delays, however they fail to quantify what a serious delay is. Two experimental set-ups were designed in order to present the computational experience with the model. The scale of the experiments is shown in Table 3.4. In some experiment instances, they reduce the available capacity by more than 85%, before an infeasible solution is obtained. In addition, they vary the capacity to see the distribution of AH and GH delay in congested airspace.

The variations of the ATFM problem listed above were developed for the tactical phase in order to manage delay. Bolić et al. [6] propose a mathematical adaptation of the Bertsimas et al. [5] that would be used in strategic flight planning. As the model is applied in the strategic phase, departure and arrival times earlier or later than the requested ones may be assigned. As a result there is no longer talk of "delay" but rather of "shift" from the requested time. When managing "shift", airborne holding and speed control are no longer options, as these management techniques are available only during operations.

The model makes use of a route based formulation instead of a sector formulation. Routes are constructed through clustering of aircraft flows from historical data from two weeks prior to the data used for the computational experiment. A route was considered viable when the points where the distance between any adjacent route is maximal measured a minimum of 20km. The formulation is emphasised by the choice of decision variable, defined by Eq. (3.5). The time constraint is now explicitly a time fix: the departure time of an aircraft from an airport.

$$x_r^f = \begin{cases} 1 & \text{, if flight } f \text{ departs at time period } t \text{ along route } r \\ 0 & \text{, otherwise} \end{cases} \tag{3.5}$$

The model can solve for two objective function: a shift-minimisation model (SMM), in which the model minimises the sum of the negative departure and positive arrival shifts per flight or a cost-minimisation model (SMC), in which the model minimises the strategic operational costs. The shift is measured from a baseline plan for each flight which is the minimum duration route and similarly the cost is measured from the minimum cost route. These baseline scenarios are determined by applying the same model but without capacity constraints at the airport.

3.5. Temporal interval

Although strategic and pre-tactical flight distribution to manage air traffic flow is widely encouraged, predictions and forecasts are not perfect, so flexibility is still needed. Therefore, mathematical models that treat the temporal element of 4D trajectories as a time interval are used to manage air traffic flow constraints. These time intervals are variations of the target windows presented in Section 3.3 in which the spatial constraints were dropped.

Corolli et al. [11] extended the ATFM model to identify a time window for each aircraft in the network to execute a phase of its flight taking off, landing and sector entering. Therefore instead of having a time period in which to carry out a phase of flight, the aircraft now has a set of contiguous time periods called a time window. The width of a time window can be a minimum of one time period or a maximum of three time periods. Unlike the model on which it is based, the time period has a physical dimension of five minutes. However, regarding the choice of maximum time window width, although again it is not explicitly mentioned,

one can assume that it is based on the fact that within the current ATM system a flight is considered delayed only after 15 minutes of deviation from the scheduled arrival or departure time.

The model consists of a two-step approach based on a mixed integer programming formulation. It first determines the sets of time windows that minimise the ATFM delay and then chooses the set that maximises the total width of the time windows. For a flight f the total delay cost is defined as the sum of the departure and arrival delay costs. The second step is necessary in order to offer the ATM stakeholders the maximum flexibility in their operations.

Sector and airport capacity are no longer modelled per time period, but per capacity period which can consist of a maximum of three time periods. The model requires three decision variables: two to fix the start and the end of a time window and one to check if a flight has entered a sector during a capacity period. Eq. (3.6),Eq. (3.7) and Eq. (3.8) define the decision variables of the model. This increase in decision variables and the need to satisfy two objectives cause this mathematical model to be computationally expensive. Therefore comparing the computational time of the regional size test problem of Bertsimas et al. [5] with that of this mathematical model, where in the experiment the en-route capacity is decreased by a factor of 95%, the number of flights by 90% and the number of sectors by 80%, the difference in average computational time is less than 20%.

$$wi^f_{j,t} = \begin{cases} 1 & \text{, if time window for flight } f \text{ in sector } j \text{ is opened by time } t \\ 0 & \text{, otherwise} \end{cases} \tag{3.6}$$

$$wf^f_{j,t} = \begin{cases} 1 & \text{, if time window for flight } f \text{ in sector } j \text{ is closed by time } t \\ 0 & \text{, otherwise} \end{cases} \tag{3.7}$$

$$co^f_{j,h} = \begin{cases} 1 & \text{, if flight } f \text{ enters sector } j \text{ during capacity period } h \\ 0 & \text{, otherwise} \end{cases} \tag{3.8}$$

The authors define critical flights as flight that get assigned a five minute time window at the departure and arrival airport. This definition is not ideal since a flight can get assigned a three period time window at the arrival and departure airport, but one period time windows in its en-route sectors. Therefore before a flight is labelled as critical a complete analysis of the width of time windows throughout the flight should be considered. However, there is no analysis into the distribution of the time windows en-route. The width of the assigned time windows depends on the available capacity en-route and at the airports. The higher the capacity, the larger the share of 15 minute time windows at the airports and the less delay there is in the system.

Due tot the large computational time of the former model, Castelli et al. [9] proposed an alternative model that also uses time windows for added flexibility in operations. This mathematical model makes use of the solution from Bertsimas et al. [5] to fix the opening time period of the time window, while a second integer programming model takes as input the solution and determines the width of the time windows, such that the total width of the time windows is maximised. The disadvantage here is that the time window can only be extended forward in time limiting the way flexibility is introduced in the system.

The model makes use of one decision variable to determine the closing time for a time window, which is given by Eq. (3.9). The objective function tries to maximise, in a fair way, the total number of periods assigned to time windows. Therefore, the notion of delay completely disappears from this mathematical formulation. The minimum and maximum width of a time window and the duration of the time period are the same as in Corolli et al. [11].

$$w^f_{j,t} = \begin{cases} 1 & \text{, if time window for flight } f \text{ in sector } j \text{ is still open at time } t \\ 0 & \text{, otherwise} \end{cases} \tag{3.9}$$

A difference between this model and that used to obtain the ATFM solution that fixes the starting time period of each TW is the way in which capacity is modelled. In the latter of the two the capacity per sector in a period of time is defined as the number of aircraft that can be in that sector in a period of time, whereas in the former capacity per sector in a period of time is defined as the number of aircraft allowed to enter the sector in that period of time. Given this new definition of capacity, the authors proposed three different criteria to compute the capacity utilization. Strict use of resource allocation means that there will be less flexibility in the system, meaning more flights have only 5 minute time windows. The authors seem satisfied

that on average the capacities are respected 99.8% of the time, however this means the algorithm does not achieve its goal since there are still capacity and demand imbalances.

The model was tested on a problem size comparable to the national size of Bertsimas et al. [5]. The model proposed in this paper requires only 40 seconds on average, however the total time to obtain the set of time windows is actually 783, since one first has to solve the ATFM problem to fix the start of the time windows. The limitation here is that the authors fail to mention what the assumed nominal capacity is, but it could be the same as the computational experiment of Bertsimas et al. [5]. The level of available capacity was varied between 10% to 100% of the nominal value to determine the distribution of time windows both en-route and at the airport, where critical flights in this case are flights that only have time windows of 5 minutes.

There mathematical models of Bertmimas and Stock Patterson [4], Bertsimas et al. [5], Corolli et al. [11], Castelli and Pellegrini [8] all have one limitation in common and that is that they have all been analysed on random air traffic scenarios, in which all sectors have the same dimensions and require the same amount of time to be transverse and the airports are sparsely distributed in the airspace grid. The model of Bolić et al. [6] accounts trough its route formulation the fact that different sectors take a different amount of time to cross. No analyses was ever performed on the probability of hitting the time constraints generated by these optimisation models in an operational context, since it would require a more microscopic approach in which the dynamics of an aircraft are considered.

Table 3.4 provides an overview of the computational set-up of each model presented in this section and Section 3.4. Except for the model of Bertmimas and Stock Patterson [4], which has been designed for a tactical planning phase and takes roughly eight hours to solve, all the remaining models could be applied within the planning phase they are designed for.

Gatsinzi et al. [20] attempted to formulate a flow management problem focused on pre-tactical de-conflicting of traffic. They propose an optimisation model whose objectives is to maximise the total number of expected conflicts removed through subliminal speed changes and to minimise the total amount of speed changes used for conflict resolution. They derive a minimum required separation time interval of 9.5 minutes when aircraft share a common 3D point in their trajectories based on the accuracy of their aircraft dynamics model. The airspace is modelled as a set of nodes and links, where the nodes are airports and the links are 4D planned trajectories. However, the model was only tested on a small test case: a pair of aircraft and one junction and it assumes that aircraft are flying their great circle distance. Therefore, the limitation of the model comes from its test-bed size.

Table 3.4: Experiment set-up and computational experience with the ATFM mathematical models with and without target windows.

Model		**Airports**	**Hub Airports**	**Sectors**	**Flights**	**Time horizon [h]**	**Capacity en-route**	**Computational time [s]**
Bertmimas and Stock Patterson [4]		18	-	305	1002	8	-	29,920
Bertsimas et al. [5]	Regional Size	20	10	113	3000	5	71	305
	National Size	30	10	145	6475	5.5	130	743
Bolić et al. [6]	SMS	204		1182	29270	24	-	250
	SMC	204		1182	29270	24	-	306
Corolli et al. [11]		5	3	25	300	3	11	257
Castelli et al. [9]		30	10	145	6475	4.2	-	40 s (+ min. 743 s)

4

Planning under uncertainty

Uncertainty has been defined in the past as having partial or limited knowledge about the existing state or future outcome of a system. In literature on uncertainty in the ATM system, there are numerous definitions, classifications and sources of uncertainty listed. Section 4.1 presents the types of uncertainty and classifications in ATM. The sources of uncertainty in the ATM system depend on weather the model in question focuses on the prediction of one trajectory or a network. This chapter, first presents models that have made effort to include uncertainty in the trajectory planning in section 4.2. Methods that model and incorporate uncertainty in models that aim to satisfy the demand and capacity balance in ATM networks are scarce, but the most relevant ones are presented in section 4.3.

4.1. Types of uncertainty in ATM

Vazquez and Rivas [43] defines four broad types of uncertainty in the ATM context: data, operational, equipment and weather uncertainty. Data uncertainty typically refers to a reduced level of confidence in the values of some parameters. This type of error can be due to imperfect aircraft performance models or unknown initial conditions. Operational uncertainty is concerned with the human factor in trajectory execution and how decisions made by one human factor effect the entire trajectory. Equipment uncertainty is represented by the error in FMS calculations or in the probability of its failure. The author chooses to classify weather uncertainty separately from data uncertainty to emphasis the importance of this type of data uncertainty in the ATM system. Weather data is typically used by both airlines and ANSP in flight planning throughout all planning phases and despite the increasing accuracy in forecasts, there is an element of uncertainty in all predictions. This uncertainty is typically due to: unknown in the initial conditions and necessary approximations in the construction of a numerical model of the real atmospheric system.

A second classification of uncertainty sources was proposed by Mondoloni [30], in which uncertainty exists due to the input errors or due to the use of a simplified aircraft performance model. Input errors are represented by any uncertainty related to the four categories described before: data, operational, equipment and weather. In the remainder of the paper, this classification will be used.

TBO is paving the way for more predictable air traffic management by supporting the sharing of information among ATM stakeholders through SWIM. This is expected to improve the flight planning process, however uncertainties will still be present since information exchange between stakeholders can never be instantaneous or continuous. One strategy in mitigating uncertainty is through the enhancement of the strategic flight plans with predictions/forecasts from the day of operation. The purpose of this is not to eliminate uncertainty, as this is not possible, but to reduce the need for tactical decisions by incorporating what is known about the uncertainty into input parameters and variables. Delay management techniques include, as already described in chapter 3, ground holding, airborne holding, speed control and rerouting.

Models that deal with planning the ATM system and simultaneously consider the uncertainty in the planning phase for which the model is designed, typically use a probability and statistic framework. Input parameters in the network optimisation or trajectory prediction model are modelled as random variables to capture the potential variations in the future trajectory of an aircraft.

4.2. Trajectory predictions subject to uncertainty

In most research for predicting an individual aircraft trajectory, the problem involves a source of uncertainty, typically an input parameter or variables, modelled as a random variable and an aircraft performance model through which the trajectory is calculated deterministically, by sampling from the random variable from its underlying distribution. Typically, these models consider a combination of the uncertainty types described by Mondoloni [30]: input and aircraft performance model uncertainty. The most common type of input uncertainty is typically weather data uncertainty. Operational uncertainty is not considered since it requires information on actions that are applied tactically by humans, which makes them difficult to model using probability theory. Equipment uncertainty, even in the context of TBO, would be hard to model, since airlines and aircraft manufacturers would have to share valuable information.

The first study to tackle the problem of trajectory prediction subject to uncertainty was addressed by Crisostomi [12] and combined probabilistic Monte Carlo methods and deterministic worst-case methods. The model is designed to be used by ATC on ground and is developed using the aircraft performance model developed by the EUROCONTROL Experimental Centre in BADA. The aim is to obtain a an empirical distribution which characterizes the most probable future trajectories and which can be used to compute estimates such as the expected time of arrival. They performed trajectory prediction for an aircraft on a leg of flight composed by the following three phases: an initial phase in level flight at 30000 ft, followed by a descent to 10000ft and a final phase again in level flight at 10000ft. The uncertainties in the prediction of the aircraft trajectory considered in this case are due to: the lack of knowledge of the exact mass of the aircraft in the prediction model, from the errors between the predicted and the actual winds encountered by the aircraft and from the observation errors, which are errors are in in the radar observations and aircraft speed observations. Navigation errors are assumed null in this study. The choice of distribution for each source of uncertainty is:

- Radar observations. Gaussian density function with zero mean and variance σ^2= 500 m^2 truncated at 2σ.
- Speed observations. Gaussian density function with zero mean and variance σ^2= 10 m/s truncated at 2σ.
- Wind . The wind is modelled as having two components: a nominal one, which corresponds to the predicted wind, plus an additive component, which corresponds to the prediction error. Wind is assumed constant at constant altitude. The chosen model is a multivariate Gaussian distribution with correlation matrix which reproduce the vertical correlation of the wind.

Rivas et al. [36] proposed two simulation-based approaches to trajectory prediction subject to weather uncertainty, that could be used in the trajectory planning process. They developed the methodology at an individual trajectory level, where they modelled the influence of weather on the aircraft state and used an aircraft performance model to determine the impact it has on the predicted trajectory. This study focuses on the effect of wind velocity uncertainty on the aircraft ground speed. The ground speed is used to study the fuel consumption in cruise flight. The result is a probability distribution of the fuel consumption. As a source of wind uncertainty they use *Ensemble Weather Forecasts* (EWF), which try to reduce the uncertainty in weather forecasting due to initial conditions and approximations in the model, by generating trough the deterministic forecast model and repeated simulation, a set of forecasts representing the range of possible weather realisations. Typically a collection includes 10 to 50 weather forecasts, called members, depending on the source used. Another weather parameter that can be modelled in a similar way is temperature. The simplified aircraft performance model consists of only the mathematical description of the motion of an aircraft in the vertical plane in cruise flight.

To obtain the probability distribution of the fuel consumption, they use two approaches one called ensemble trajectory prediction and the other probabilistic trajectory prediction. In the first method, for each member of the EWF, the ground speed is calculated and an associated cruise fuel consumption obtained through the deterministic aircraft model. The probability distribution can then be derived based on frequency histograms of fuel consumed. In the second case, one first assumes a wind distribution from the available wind data, from which the ground speed distribution is computed, and then makes use of the equation of motion to determine the fuel consumption probability density function.

The advantage of the ensemble trajectory predictor is that it can easily compute other trajectory parameters by rearranging the kinematic equations to make the dependent variable the end parameter. Then one only needs to make an assumption about the distribution of the calculated parameter. However, the disadvantage is that it is very expensive in computational terms when there are more sources of uncertainty considered. On the other hand the challenge in the probability trajectory predictor comes in the type of dis-

tribution chosen for the initial state that is subject to uncertainty, which is not always trivial. In this study the ground speed follows uniform continuous distribution as described by Equation 4.1, where V_{g_j} is the aircraft ground speed in a cruise sector j in the interval $\left[V_{g_{j,m}}, V_{g_{j,M}}\right]$ where $V_{g_{j,m}}$ and $V_{g_{j,M}}$ are estimated from the sample by using the method of moments for a sector.

$$f_{V_{g_j}}\left(V_{g_j}\right) = \begin{cases} 1/\left(V_{g_{j,M}} - V_{g_{j,m}}\right), & V_{g_j} \in \left[V_{g_{j,m}}, V_{g_{j,M}}\right] \\ 0, & V_{g_j} \notin \left[V_{g_{j,m}}, V_{g_{j,M}}\right] \end{cases} \tag{4.1}$$

$$E\left[V_{g_j}\right] = \left(V_{g_{j,M}} + V_{g_{j,m}}\right)/2 \tag{4.2}$$

$$\sigma\left[V_{g_j}\right] = \left(V_{g_{j,M}} - V_{g_{j,m}}\right)/(2\sqrt{3}) \tag{4.3}$$

Franco et al. [19] tested the methodology of trajectory prediction for the trajectory planning process by modelling the ground speed variable as a Log-Normal distributions, described by Equation 4.4, instead of uniform distributions. In addition the model assumed account several wind forecasts trough out the cruise phase, rather than a fixed wind distribution for the whole cruise. In order to take into account that the aircraft has to fly through areas of different look-ahead time, several forecasts are considered, released at the same time with time steps of 6 hours. The authors provide the following example: if the forecasts are released at 6:00, the flight departure time is 11:00 and expected landing is at 19:00, and the prediction is made at 8:00, the model will make use of the forecast at 6 and 8. Instead of determining only the variation in fuel consumption of the trajectory due to uncertainty the model considers the effect of weather uncertainty on flight time as well. The probabilistic trajectory predictor consists in the sequential application of the method: first, the probability density function of the ground speed in each cruise segment ($\overline{V}_{g_j}/V \sim \log N\left(\mu_j, \sigma_j\right)$) is evolved to give the PDF of the flight time in each segment; then, all of these density functions give the probability density function of the total flight time; finally, the total flight time gives the of the aircraft fuel consumption to be distributed as a Log-Normal continuous variable.

$$f_{\overline{V}_{g_j}}\left(\overline{V}_{g_j}\right) = \begin{cases} \frac{1}{\overline{V}_{g_j}\sigma_j\sqrt{2\pi}} \exp - \frac{\left[\log\left(\overline{V}_{g_{j,i}/V}\right) - \mu_j\right]^2}{2\sigma_j^2}, & \overline{V}_{g_j} > 0 \\ 0, & \text{otherwise} \end{cases} \tag{4.4}$$

$$\mu_j = \frac{1}{n}\sum_{i=1}^{n} \log\left(\overline{V}_{g_{j,i}}/V\right) \tag{4.5}$$

$$\sigma_j = \sqrt{\frac{1}{n-1}\sum_{i=1}^{n}\left[\log\left(\overline{V}_{g_{j,i}}/V\right) - \mu_j\right]^2} \tag{4.6}$$

Gonz et al. [21] proposes an optimisation model that can be used to plan wind-optimal aircraft trajectory at pre-tactical level. The optimisation uses an optimal control technique called neighbouring optimal control based on analytical optimal control. As with the previous two models, the weather information comes from EWF. The aircraft performance model used to derive the dynamical system of the aircraft is based on BADA 3.0 model (from Eurocontrol [18]). BADA 3.0 is a standard aircraft performance model widely used in the ATM community for research as it covers the nominal part of a great number of aircraft operational envelopes. The methodology proposed is also similar to the last study but instead of performing just a simulation-based analysis, an optimisation step is included. This is an optimal control problem, where all trajectories are considered simultaneously. A trajectory ensemble is obtained by calculating in a deterministic manner each trajectory based on a control law and uncertainty parameters which are modelled as random variables. The distribution is used for the wind uncertainty is not indicated. The control law minimises the weighted sum of the average flight time and flight time dispersion.

Álvaro Rodriguez-Sanz et al. [45] developed a trajectory prediction model that considers input data and weather uncertainty. This is a simulation-based approach with Monte Carlo method in which the trajectory calculation is deterministic and done using a three degrees of freedom aircraft performance model. The aircraft performance model in this case is based on the BADA 4 model. The advantages of using bada 4 over bada 3 are the increase in accuracy in the physical relations in some sub-models and inclusion of the entire aircraft envelope. The goal of the simulations is to define the uncertainty in the time the aircraft arrives at a checkpoint and to identify which uncertainty parameters have the greatest influence on the uncertainty window.

Unlike the previous research in which the performance models used are not validated, this model is, with real flight trajectories representative of the case study considered. The authors found only a 7% difference in the real trajectory and that predicted with the performance model. Monte Carlo methods were used and therefore the uncertainty parameters were modelled as random variables and sampled from their respective distributions. In Table 4.1, the input parameters modelled as random variables and the distributions chosen to capture parameters are listed.

Table 4.1: Uncertainty parameters considered in Álvaro Rodriguez-Sanz et al. [45] and modelling choice.

Influence Parameter	**Uncertainty modelling**
Temperature and atmospheric variables	Normal distribution
Initial Mass	Uniform distribution
Fuel consumption	Normal distribution
Wind	Normal distribution
Navigation systems	Normal distribution

4.3. Traffic planning subject to uncertainty

Deterministic air traffic flow management decisions as those generated by the algorithms in chapter 3, often result in capacity and demand imbalances or conflicts, because the inherent uncertainties in flight prediction are not considered. Vazquez and Rivas [43] mentions that there are ongoing studies into the development of stochastic models that optimise for air traffic flow management constraints.

One such research is that of Clarke et al. [10], which proposed a stochastic trajectory optimisation to solve the ATFM, which uses probabilistic capacity information for a volume of airspace to dynamically route aircraft destined to the sector. The optimisation is based on a linear integer programming model, in which the objective is to minimise the sum of ground-delay, speed-change costs, air-holding and diversion costs. Capacity is defined as the maximum number of aircraft that can enter a volume of airspace. The probabilistic capacity information is obtained from weather forecasts, through a model that aims to capture any existing relationships between weather and capacity for a given volume of airspace. The weather-capacity model is based on Monte-Carlo simulations of the traffic flow using a conflict-resolution algorithm and a range of possible weather realisations. The weather realisations come from the probabilistic weather forecasts, such as the 1-6 hour National Convective Weather Forecast (NCWF-6), which provide a depiction of future locations of existing convective hazards for lead times of 30, 60, 90, and 120 min in 1-6h given in a probabilistic sense. The outcome of the model is the probability distribution of capacity for the airspace over a given time interval obtained based on different levels of arrival rate and distribution.

The uniqueness of the model comes form the fact that it simultaneously address two problems. One one hand, it deals with the planning of demand and capacity, by determining the number of aircraft to send towards that airspace, and considers conflict resolution when setting the capacity of a sector.

5

Simulation environments in ATM research

The models used for strategic and pre-tactical flight planning have to be evaluated at a tactical level, in order to understand the impact of network strategies on individual flights. Therefore, simulation environments to test out the solution methods must be developed. This chapter presents some of the simulation environments used in the ATM community and their associated limitations.

There are two different categories of simulations: real-time and fast-time atm simulations according to Ellerbroek and Hoekstra [16]. The real-time simulators are designed for human-in-the-loop experiments and typically these experiments consider only a restricted part of traffic in a network, such a the terminal manoeuvre area. This type of simulation environment tends to focus on the ATCo workload, scenario acceptability or interaction between the human and ATM technologies or between ATM stakeholders. Typically this experiments make use of the different working stations of the stakeholders. The second type of simulation environment, the fast-time simulations are designed for batch-simulation with the goal of assessing variables that indicate productivity of the ATM system such as flight time and fuel consumption of individual aircraft under the effect of airspace capacity, environmental condition, number of conflicts etc. Fast-time simulations allow reliable and economically evaluations of models, the type of simulation environment is needed to evaluate the ATFM from chapter 3.

There is a wide variety of fast-time simulation tools that are accepted by the ATM community: on one hand there are commercial off-the-shelf tools like: AirTop Air [1], which is maintained by EUROCONTROL, and on the other hand there are open-source simulators like BlueSky Hoekstra and Ellerbroek [25], developed at TU Delft. Most simulators are based on similar complex aerodynamics or total energy equations, despite this fact they may produce different outputs for the same input due to the difference in implementation or assumptions. Therefore, in order to create uniformity in the results on ATM research, BlueSky was developed. It facilitates the comparison of the results of different studies with the same metrics, traffic scenario and simulation tools and in addition can makes use of the BADA 3.0 performance model. The advantage of using an open-source simulator, such as BlueSky, is the flexibility of adapting it to each application.

The key enabler of trajectory-based operations is the aircraft FMS. Enea and Porretta [17] mentioned that the pilots from the first i4D flight though it is essential that FMS be enhanced to facilitate time adherence in 4D trajectories, through datalink communication and increased trajectory prediction for the RTA function. Therefore the fast-time simulator should support some of the existing FMS functions and possible additional logic that could be used in time window adherence. None of the existing simulators currently have an advance FMS function that could potentially support the evaluation of the hitting probability of time constraints. This could easily be implemented in an open-source simulator, such as BlueSky, whereas a commercial simulator would require a lot of time to develop such a function. However, the cost associated to using only open-source data is the loss in the accuracy of the model due to more build in assumption. One of the only studies that tried to evaluate the impact of a time of arrival controller in fast-time simulations on the time of arrival at a target window was Margellos and Lygeros [29], but used a simple two state model to represent the aircraft dynamics.

The simulation environment for evaluating the models at a the tactical planning phase should include uncertainties. In the past, several models have considered introducing uncertainty in trajectory prediction with the scope of evaluating the probability of hitting a time window, but typically made use of simplified aircraft dynamics. Two such examples are those of Castelli et al. [9] and Margellos and Lygeros [29]. Castelli

et al. [9] made an attempt to study the utilisation of airspace capacity when aircraft aim hit time windows. A departure time is randomly assigned to each flight within its departure time window and the sequence of time windows used by the aircraft tracked. The probability density function of the departure time is either: a) uniform, in which all time windows can be selected with the same probability b) triangular, where the first time period has the highest probability and the last one the lowest probability, and c) mixed function, where the first time window has a 50% probability and the remaining two have 25%. Margellos and Lygeros [29] analysed the time window hitting probability in 50 flights in a fast-time simulation which included 4 sources of uncertainty: a) wind b) aircraft mass c) sector entry time, and d) nominal speed uncertainty.

Bibliography

[1] En-route simulation. URL http://airtopsoft.com/en-route-simulation/.

[2] Peter Belobaba. The Airline Planning Process. *The Global Airline Industry*, pages 153–181, 2009. doi: 10.1002/9780470744734.ch6.

[3] I. Berechet, F. Debouck, L. Castelli, A. Ranieri, and C. Rihacek. A target windows model for managing 4-d trajectory-based operations. In *2009 IEEE/AIAA 28th Digital Avionics Systems Conference*, pages 3.D.2–1–3.D.2–9, Oct 2009. doi: 10.1109/DASC.2009.5347513.

[4] Dimitris Bertmimas and Sarah Stock Patterson. The Air Traffic Flow Management Problem with Enroute Capacities. *Encyclopedia of Social Measurement*, pages 925–931, 1998. doi: 10.1016/b0-12-369398-5/00534-x.

[5] Dimitris Bertsimas, Guglielmo Lulli, and Amedeo Odoni. An Integer Optimization Approach to Large-Scale Air Traffic Flow Management. *Operations Research*, 59(1):211–227, 2011. ISSN 0030-364X. doi: 10.1287/opre.1100.0899.

[6] Tatjana Bolić, Lorenzo Castelli, Luca Corolli, and Desirée Rigonat. Reducing ATFM delays through strategic flight planning. *Transportation Research Part E: Logistics and Transportation Review*, 98:42–59, 2017. ISSN 13665545. doi: 10.1016/j.tre.2016.12.001.

[7] J. Martin Freiherr von Castell. *Analysis of the influence of the Air Traffic Management initiatives SESAR and NextGen on Airline Operations Control Centers' workflows*. PhD thesis, Berlin Institute of Technology, 2014.

[8] Lorenzo Castelli and Paola Pellegrini. An AHP analysis of air traffic management with target windows. *Journal of Air Transport Management*, 17(2):68–73, 2011. ISSN 09696997. doi: 10.1016/j.jairtraman.2010.05.006. URL http://dx.doi.org/10.1016/j.jairtraman.2010.05.006.

[9] Lorenzo Castelli, Luca Corolli, and Guglielmo Lulli. Critical Flights Detected with Time Windows. *Transportation Research Record: Journal of the Transportation Research Board*, 2214(-1):103–110, 2011. ISSN 0361-1981. doi: 10.3141/2214-13. URL http://trb.metapress.com/openurl.asp?genre=article&id=doi:10.3141/2214-13.

[10] John-Paul B. Clarke, Senay Solak, Yu-Heng Chang, Liling Ren, and Adan E. Vela. Air traffic flow management in the presence of uncertainty. *Eighth USA/Europe Air Traffic Management Research and Development Seminar (ATM2009)*, 2009.

[11] L. Corolli, L. Castelli, and G. Lulli. The air traffic flow management problem with time windows. *4th Internation*, pages 201–207, 2010. URL http://www.cats-fp6.aero/pub/CATS_ICRAT2010.pdf.

[12] E Crisostomi. Combining Monte Carlo and worst-case methods for trajectory prediction in air traffic control: a case study. *Guidance, Control*, 2008. URL http://www-control.eng.cam.ac.uk/~al394/ACA09.pdf.

[13] Customer Services AIRBUS. Cost Index. Technical Report II, 1998.

[14] Veronica Dal Sasso, Franklin Djeumou Fomeni, Guglielmo Lulli, and Konstantinos G. Zografos. Incorporating Stakeholders' priorities and preferences in 4D trajectory optimization. *Transportation Research Part B: Methodological*, 117:594–609, 2018. ISSN 01912615. doi: 10.1016/j.trb.2018.09.009. URL https://doi.org/10.1016/j.trb.2018.09.009.

[15] David De Smedt and Gerhard Berz. Study of the required time of arrival function of current FMS in an ATM context. *AIAA/IEEE Digital Avionics Systems Conference - Proceedings*, pages 1–10, 2007. doi: 10.1109/DASC.2007.4391837.

[16] Joost Ellerbroek and Jacco Hoekstra. AE4321 Air Traffic Management Surveillance, 2018.

[17] Gabriele Enea and Marco Porretta. A comparison of 4D-trajectory operations envisioned for Nextgen and SESAR, some preliminary findings. *28th International Congress of the aeronautical sciences*, pages 1–14, 2012. URL http://skybrary.aero/bookshelf/books/2377.pdf.

[18] Eurocontrol. USER MANUAL FOR THE BASE OF AIRCRAFT DATA (BADA 3). Technical Report 13, 2006.

[19] Antonio Franco, Damián Rivas, and Alfonso Valenzuela. Probabilistic aircraft trajectory prediction in cruise flight considering ensemble wind forecasts. *Aerospace Science and Technology*, 82-83:350–362, 2018. ISSN 12709638. doi: 10.1016/j.ast.2018.09.020. URL https://doi.org/10.1016/j.ast.2018.09.020.

[20] Dany Gatsinzi, Francisco J. Saez Nieto, and Irfan Madani. Development of a new method for ATFCM based on trajectory-based operations. *Proceedings of the Institution of Mechanical Engineers, Part G: Journal of Aerospace Engineering*, 233(1):261–284, 2019. ISSN 20413025. doi: 10.1177/0954410017728968.

[21] Daniel Gonz, Manuel Soler, and Manuel Sanjurjo. Wind-Based Robust Trajectory Optimization using Meteorological Ensemble Probabilistic Forecasts. *DBIAB - AERO - Proceedings*, 2016(November):1–8, 2016.

[22] Sandrine Guibert and Laurent Guichard. 4D Trajectory Management using Contract of Objectives. *Journal of Aerospace Operations*, 1(3):231–248, 2012. doi: 10.3233/AOP-2012-0017.

[23] Sandrine Guibert, Laurent Guichard, and Jean-yves Grau. Human in the Loop To Assess 4D Trajectory Management With Contract-of-Objectives. *Human Performance*, pages 1–10, 2008.

[24] Sandrine Guibert, Laurent Guichard, Christoph Rihacek, and Jean Yves Grau. Result from evaluation of 4d trajectory management with contract-of-objectives. *AIAA/IEEE Digital Avionics Systems Conference - Proceedings*, pages 5–1, 2009. doi: 10.1109/DASC.2009.5347512.

[25] Jacco M Hoekstra and Joost Ellerbroek. BlueSky ATC Simulator Project: an Open Data and Open Source Approach. *7th International Conference on Research in Air Transportation*, pages 1–8, 2016. URL http://www.icrat.org/icrat/seminarContent/2016/papers/5/ICRAT_2016_paper_5.pdf.

[26] ICAO. *ICAO Doc 4444: Procedures for Air navigation Services*, volume 4444. 2016. ISBN 978-92-9258-081-0. URL http://flightservicebureau.org/wp-content/uploads/2017/03/ICAO-Doc4444-Pans-Atm-16thEdition-2016-OPSGROUP.pdf.

[27] International Civil Aviation Organisation. Time adherence in TBO. 2014. URL http://www.sesarju.eu/sites/default/files/documents/reports/WP636_Trajectory_adherence_in_TBO.pdf?issuusl=ignore.

[28] Kostas Margellos and John Lygeros. Air traffic management with target windows: An approach using reachability. *Proceedings of the IEEE Conference on Decision and Control*, pages 145–150, 2009. ISSN 01912216. doi: 10.1109/CDC.2009.5400119.

[29] Kostas Margellos and John Lygeros. Toward 4-D trajectory management in air traffic control: A study based on monte carlo simulation and reachability analysis. *IEEE Transactions on Control Systems Technology*, 21(5):1820–1833, 2013. ISSN 10636536. doi: 10.1109/TCST.2012.2220773.

[30] Stephane Mondoloni. Trajectory-based operations - Robust planning under trajectory uncertainty. *AIAA/IEEE Digital Avionics Systems Conference - Proceedings*, 2016-Decem, 2016. ISSN 21557209. doi: 10.1109/DASC.2016.7778019.

[31] Laurence H Mutuel and Pierre Neri. Initial 4D Trajectory Management Concept Evaluation. *Tenth USA/Europe Air Traffic Management Research and Development Seminar (ATM2013)*, 2013.

[32] Network Manager. ATFCM Users Manual. Technical report, 2018. URL www.eurocontrol.int.

[33] Angela Nuic and Vincent Mouillet. User manual for the base of aircraft data (bada) - revision 3.6. Technical report, European Organisation for the Safety of Air Navigation (EUROCONTROL), 2004.

[34] Angela Nuic and Vincent Mouillet. User manual for the base of aircraft data (bada) family 4. Technical report, European Organisation for the Safety of Air Navigation (EUROCONTROL), 2014.

[35] Amedeo Odoni. The Flow Management Problem in Air Traffic Control. pages 2–6, 1987.

[36] Damián Rivas, Antonio Franco, and Alfonso Valenzuela. Analysis of aircraft trajectory uncertainty using Ensemble Weather Forecasts. *European Conference for Aeronautics and Space Sciences (EUCASS)*, pages 1–12, 2017. doi: 10.13009/EUCASS2017-259. URL https://www.eucass.eu/doi/EUCASS2017-259.pdf.

[37] B. Roberson. Fuel Conservation Strategies. Technical Report Ci, 2007. URL http://www.boeing.com/commercial/aeromagazine/articles/qtr_02_10/pdfs/AERO_FuelConsSeries.pdf.

[38] SESAR. SESAR SWIM Factsheet - Connecting the ATM world, 2016.

[39] SESAR Consortium. WP2.2.2/D3 SESAR Definition Phase-Task deliverable. (July):1–214, 2007. URL https://www.eurocontrol.int/sites/default/files/field_tabs/content/documents/sesar/20070717-sesar-conops.pdf.

[40] Graham Tanner. The Principles of Flight Planning and ATM Messaging. In Andrew Cook, editor, *European air traffic Management: principles, practice and research*, pages 65–96. ASHGATE, 2007.

[41] E Ulfbratt and J McConville. Comparison of the SESAR and NextGen Concepts of Operations. *NCOIC Aviation IPT*, 1.0:22, 2008. URL http://scholar.google.com/scholar?hl=en&btnG=Search&q=intitle:Comparison+of+the+SESAR+and+NextGen+Concepts+of+Operations#0.

[42] F. J. van Schaik. *Introduction to Air Traffic Management*. Number August. TU Delft, 2010.

[43] Rafael Vazquez and Damian Rivas. Chapter 4: Uncertainty. In *Complexity Science in Air Traffic Management*, volume 1, pages 41–60. Routledge, 2016. ISBN 0471499269. doi: 10.1016/S0065-2776(07)95004-X.

[44] Randy Walter. Flight management systems. In *Digital Avionics Handbook, Third Edition*, chapter 15. 2017. ISBN 9781439868980. doi: 10.1201/b17545.

[45] Álvaro Rodriguez-Sanz, Fernando Comendador Gomezand, and Rosa Arnaldo Valdes. 4d-trajectory time windows: Definition and uncertainty management. *Aircraft Engineering and Aerospace Technology*, 91: 761–782, 2018. ISSN 0002-2667. doi: 10.1108/AEAT-01-2018-0031.

III

Further elaboration on thesis work

A

BlueSky open-source ATC simulator

Through out the research the BlueSky ATC simulator [25], developed at TU Delft, will be used. The advantage this ATM simulation tool posses over the other available options is that it is open-source, which makes it easily extensible with new features required for this research. BlueSky is build in the high-level programming open-source language Python (version 3). The simulator is available for free download an the GitHub webpage[1]. First, an overview of structure of the BlueSky simulation environment is provided in Appendix A.1.

A.1. BlueSky Structure

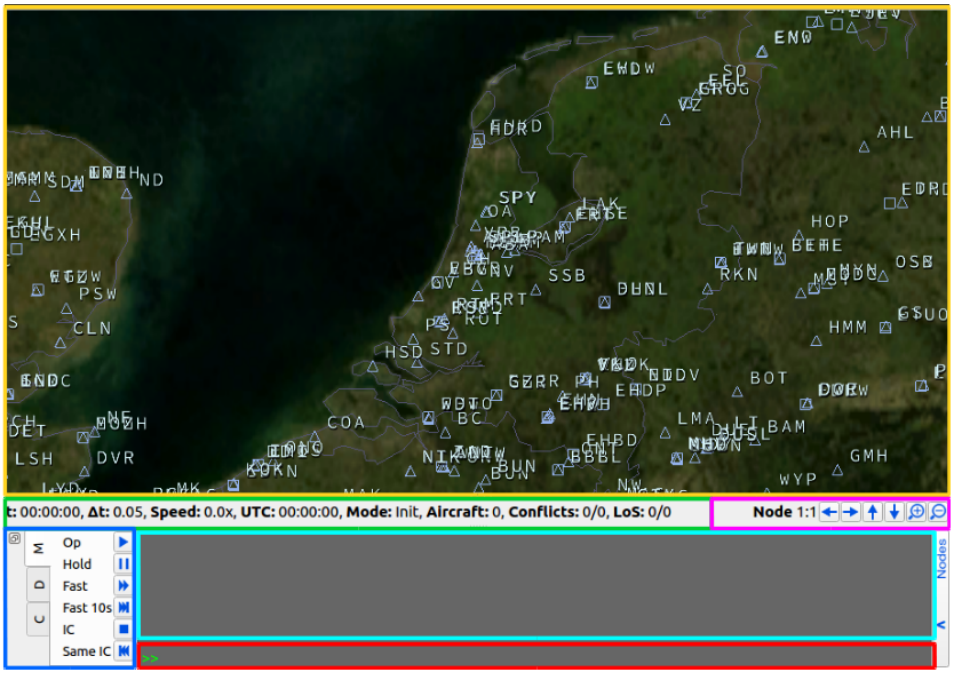

Figure A.1: BlueSky UI.

To be able to add a new functionality to BlueSky that will aid in answering the research question, the structure of the simulator is investigated. BlueSky has a modular set-up, where at the highest level sit the simulation engine and the UI modules. The simulation module is responsible for both the traffic simulation and the execution of the programme and consist of five classes: Traffic, Simulation, Stack, Tools and Screen. On the other hand, the UI allows for traffic visualisation and control over the simulation, through a command line and menus and consists of the Screen class. A screenshot of the BlueSky ATC simulator screen can be seen in Fig. A.1. The five classes previously discussed are listed below with a short explanation.

[1] `https://github.com/TUDelft-CNS-ATM/bluesky`

Traffic
The Traffic class contains all of the data related to the actual simulation, which can be the aircraft state (spacial coordinates, velocities etc.), or any other simulation aspects effecting the aircraft behaviour. The most relevant elements are simulated for this thesis research include, but are not limited to the wind model, the aircraft performance models, the navigation data base, the flight management system model and the autopilot.

Simulation
The Simulation class keeps track of the state of the simulation and manages its timing. It supports the start, hold, fast-forward and stop functionalities of the simulation.

Stack
The Stack class is used to parse user commands, given in language TrafScript, that control the simulation. TrafScript is BlueSky's personal scripting language. The commands can be used directly within the BlueSky interface, through the command line, or can be used to construct traffic scenarios as a series of commands (.scn). An exhaustive list of BlueSky commands can be found on the GitHub page.

Tools
The Tool class supports the simulation through a wide range of functionalities, such as atmospheric calculations, bearing calculations, data logging functions, etc.

Screen
The Screen class makes the interaction between the user and the program user-friendly. The user can interact with the simulation tool trough: a command line in which TrafScript commands can be inserted (red rectangle in Fig. A.1) and a menu to control the state of the simulation (start,hold,etc.) and to select the scenario file that should be simulated (blue box of the Fig. A.1). The remainder screen space is used to display the traffic (yellow), the simulation state (light green) and to control the map view (magenta).

The most important feature of BlueSky for this research is the FMS functionality. This provides the ability to define routes for aircraft in the simulation using BlueSky input files called scenario files (.scn). This information is stored within BlueSky within the Route object of the Traffic class and due to the crucial role it plays in the development of the speed control methodology, the workings are explained in detail in Appendix A.1.1. The aircraft is simulated to move through waypoints using the *Lateral Navigation* (LNAV) and *Vertical navigation* (VNAV) which constitute the autopilot.

A.1.1. Route

The route is made up of a series of waypoints defined at specific latitude and longitude coordinates. In addition, for each waypoint there is an associated flight level that the aircraft must pass the waypoint at. The route data is contained within the Route object of each aircraft. In addition to the required properties: latitude, longitude and altitude, a speed can be assigned to use on the leg towards the next waypoint and a waypoint type, which is either fly-by, fly-over or take-off. However, for this reasearch a speed control methodology for time windows adherence is used and as a result no speed requirements are to be imposed at the waypoints. The default waypoint type is a fly-by.

A waypoint can be added to the route of the aircraft via the "ADDWPT" command. Waypoints that are already available within the BlueSky navigational database can be called directly, via the waypoint name. A custom geographical waypoint can be created in the database using "DEFWPT" command with a custom name and a latitude/longitude pair. The altitude, speed, type of waypoint (fly-by/fly-over/take-off) are optional commands that can be passed after the defaults seen above. By default any new added waypoint is inserted directly at the end of the route, however one can also select a specific waypoint within the route after which to insert the new waypoint by passing its name at the end of the "ADDWPT" command. The use of these commands within a scenario file can be found in Listing A.1.

Listing A.1: An example of a .scn file used containing commands used in the route construction

```
00:00:00.00>HOLD
00:00:00.00>DATE 09 09 2014 05:12:44.00
00:00:00.00>CRE ADH931, A320, 37.71, 15.46, 21.58, FL150, 310
0:00:00.00>DEFWPT wpt_0 37.71 15.46
0:00:00.00>DEFWPT wpt_1 40.91 12.96
0:00:00.00>DEFWPT wpt_2 42.99 10.19
```

```
0:00:00.00>ADDWPT ADH931,wpt_0,FL150
0:00:00.00>ADDWPT ADH931,wpt_1,FL360
0:00:00.00>ADDWPT ADH931,wpt_2,FL250
0:00:00.00>LNAV ADH931 ON
0:00:00.00>VNAV ADH931 ON
00:00:00.00>OP
```

The aircraft follows the route one waypoint at a time using the autopilot functionalities LNAV and VNAV. The Route object keeps track of the active waypoint and the flight-leg which the aircraft is currently on.

A.1.2. Lateral Navigation

The LNAV functionality of BlueSky is activated through the "LNAV ON" command and when it is in use the aircraft travels along the route from one waypoint to another. In the case of a fly-by waypoint, the flight has reached its active waypoint in the route when the remaining distance to it is smaller than the minium distance to start the turn onto the next flight-leg d_{turn}. This distance is defined by the difference between the current aircraft heading (ψ_j) and the heading of the next flight leg (ψ_{j+1}) and calculated using Equation (A.1).

$$d_{\text{turn}} = \left| R_{\text{turn}} \cdot \arctan\left(\frac{1}{2}(\psi_j - \psi_{j+1})\right)\right| \tag{A.1}$$

Using Eq. (A.2) the turn radius is obtained, where a default bank angle ϕ is used based on the aircraft type and flight phase. For the cruise phase the default is 25°. When the turn is initiated, the active waypoint in the route is switched to its successor.

$$R_{\text{turn}} = \frac{V_{TAS}^2}{\tan\phi \cdot g_0} \tag{A.2}$$

A.1.3. Vertical Navigation

The VNAV functionality is triggered by the use of the "VNAV ON" command as seen in Listing A.1. In the cruise phase, VNAV uses a simple logic which ignores and looks beyond waypoints along the route that do not have an altitude constraint until it finds the first altitude constrained waypoint. In the case the aircraft has to climb towards it, it does so as soon as possible after the previous altitude constraint and in case it has to descent such that a constant climb or glide angle of 0.05° is maintained.

B

Fuel Consumption Estimation Model

The future implementation of the TW concept of operations is dependent on the willingness of airlines to cooperate with the new procedure supported by the Network Manager. Therefore, understanding the impact of the TW adherence on the fuel consumption during flight is crucial. As a result the fuel consumption determination process used in the project must be understood.

To estimate the amount of fuel consumed by each aircraft when flying their 4D trajectories with TWs the BADA is used. BADA is one of the best known aircraft performance models, which is provided and maintained by *European Organization for Safety of Air Navigation* (EUROCONTROL). The BADA *Aircraft Performance Model* (APM) is characterized by four modules: Actions, Motion, Operations and Limitations. The Actions model includes the calculation of four forces acting on the aircraft: weight W, lift L, drag D and thrust D and the fuel consumption F, which impacts the aircraft mass m. The Motion model consists of the system of equations that describes the aircraft motion. The Operations model includes methods of operating the aircraft that are outside the boundaries of the Actions and Motion models, while the Limitations model constraint the aircraft behaviour within certain limits.

The Motion model describes the aircraft motion as well as the different ways of operating the aircraft. The base of this model is the Total-Energy Model (TEM), which is shown in Eq. (B.1), where T is the thrust acting parallel to the aircraft velocity vector, D is the aerodynamic drag, m is the aircraft mass, $g_0 = 9.81\,\mathrm{m\,s^{-2}}$ is the gravitational acceleration, V_{TAS} is the true airspeed, h is the altitude and $\frac{d}{dt}$ indicates a derivative with respect to time. The equation equates the rate of work done by the forces acting on the aircraft to the rate of increase in potential and kinetic energy.

$$(T-D)V_{TAS} = mg_0\frac{dh}{dt} + mV_{TAS}\frac{dV_{TAS}}{dt} \tag{B.1}$$

Equation (B.2) is the second equation of the Motion model, which describes the variation of mass during flight, where m is the aircraft mass and F is the fuel consumption defined in $\mathrm{kg\,s^{-1}}$ and dt is the simulation time step. In this study, the time step is set to 1 s.

$$m = -F\,dt \tag{B.2}$$

From the general formulation of the TEM in Eq. (B.1), the two independent control inputs are identified that can be used to affect the aircraft performance. These inputs allow any two of the three variables of thrust, speed or rate of climb or descent (ROCD) to be controlled, while the other is determined through Eq. (B.1). The resulting control laws are:

Speed and Throttle Controlled This assumes that the speed and thrust are independently controlled, which means Eq. (B.1) can be used to identify the ROCD. The throttle in this case is set to a fixed position and the V_{TAS} is maintained constant.

ROCD and Throttle Controlled In this case Eq. (B.1) is used to determined the resulting V_{TAS}.

Speed and ROCD Controlled In this case Eq. (B.1) is used to determined the necessary thrust, which must be within the available limits for the desired ROCD and V_{TAS} to be maintained.

The APM is available within two levels of accuracy: the 3 family and the 4 family. The BADA 3 model is widely accepted and used by the ATM community since it provides credible modelling of the aircraft be-

haviour within the nominal part of the flight envelope. On the other hand, BADA 4 relies on the use of commercial reference data to model the entire aircraft operational envelope. It overcomes the limitations of BADA 3 in modelling the thrust in relation to speed and in estimating the fuel flow [25]. This makes this version of BADA subject to strict licensing since it supports the modelling of operations outside the nominal region of the flight envelope.

In this research, speed variations are used during the enroute phase of the flight as one of the main enablers of the TW concept of operations. The BADA 4 provides a higher precision for the thrust calculation of jet engines, by modelling its dependency on airspeed. Therefore this model would offer a higher precision on the fuel consumption estimation. However, BlueSky supports only the BADA family 3 aircraft performance model. The architecture of the BADA 3 implementation in BlueSky is not compatible with the BADA 4 coefficients data files since their structure and the number of parameters available differs.

To use fuel model of BADA 4 either the implementation of the model in BlueSky is to be carried out, or the required input data to the model: the aircraft model, altitude, flight phase, temperature and speed need to be obtained. These aircraft states are available as a result of the flight simulation of operations carried out in BlueSky using in BADA 3 model. The former option reduces the precision of the fuel estimation, as it requires the use of some assumptions in the thrust model, but avoids the complexity of implementing BADA 4 in BlueSky, therefore this option was selected. To understand where certain limitations arise due to this modelling choice, the Actions model of each APM is detailed in section B.1 and Appendix B.2. The focus is on the details of the jet/turbofan model since the flights that are simulated are carried out using turbofan engines. Finally, the fuel determination process is explained in Appendix B.3, where the assumption about the throttle parameter used in the fuel determination process of BADA 4 is provided.

B.1. BADA 3 Model [33]

B.1.1. Drag force in BADA 3

The drag force in BADA 3 is determine by the drag coefficient C_D using Eq. (B.3), where ρ is air the density at the flight altitude, S is the wing surface area and V_{TAS} is the true airspeed.

$$D = \frac{1}{2} C_D S \rho V_{TAS}^2 \tag{B.3}$$

The drag coefficient C_D in consists of two components: a parasite drag C_{D0} and drag due to lift C_{D2}. The lift coefficient C_L is determined through Eq. (B.5), where m is the aircraft mass, g_0 is the gravitational acceleration and ϕ is the bank angle. The coefficients are independently specified for the nominal, approach and landing phase of flight. In nominal configuration this model does not take into account the compressibility effect at high altitudes and speeds, which means there there is only one drag polar for all conditions.

$$C_D = C_{D0} + C_{D2} \cdot C_L^2 \tag{B.4}$$

$$C_L = \frac{2 m g_0}{\rho V_{TAS}^2 S \cos\phi} \tag{B.5}$$

B.1.2. Thrust model in BADA 3

The thrust force is calculated based on five separate levels: maximum climb, nominal climb, maximum take-off, maximum cruise and descent. The maximum climb and take-off thrust $T_{\text{max climb}}$ is a function of engine type (jet, turboprop or piston) and is calculate using a different formula for each. The thrust from a jet engine is dependent only on the altitude h, while those for turboprop and piston engine are dependent on the altitude h an true airspeed V_{TAS}.

The maximum amount of thrust available during cruise is limited and is calculated as a ratio of the maximum climb thrust given in Eq. (B.6). The C_{Tcr} is a uniformly set for all aircraft at 0.95. For all engine types the maximum climb thrust can be corrected for temperature deviations from the International Standard Atmosphere (ISA) through a factor defined by ΔT_{ISA}.

$$T_{\text{max cruise}} = C_{\text{Tcr}} \cdot T_{\text{max climb}} \tag{B.6}$$

B.1.3. Fuel Consumption in BADA 3

The fuel flow f is defined by Eq. (B.7) where, η is the thrust specific fuel consumption [kg min^{-1} N^{-1}] that can be calculated through Eq. (B.8) in nominal conditions. The C_{f1} and C_{f2} are two dimensionless coefficients obtained from the BADA 3 operation performance files. The nominal fuel flow is used in all phases except for the cruise and idle descent.

$$f_{\text{nom}} = \eta \cdot T \tag{B.7}$$

$$\eta = C_{f1} \cdot \left(1 + \frac{V_{TAS}}{C_{f2}}\right) \tag{B.8}$$

Finally, C_{fcr} is a dimensionless factor provided by the aircraft manufacturers to scale the nominal fuel flow f_{nom} to the cruise norms. If no data is available on this factor, a value of 1 is assigned.

B.2. BADA 4 Model [34]

B.2.1. Drag force in BADA 4

In a similar manner, Eq. (B.3) is used to calculate the drag force in BADA 4. While in the previous model compressibility effects were ignored, BADA 4 takes them into account through the C_D specification. The drag coefficient, C_D, is calculated differently for each aerodynamic configuration and is a function of the lift coefficient C_L, obtained using Eq. (B.5), and the Mach number. The aerodynamic configuration is a combination of the high-lift devices position δ_{HL}, the landing gear position δ_{LG} and the speed break position δ_{SB}.

$$C_D = f(C_L, M, \delta_{\text{HL}}, \delta_{\text{LG}}\delta_{\text{SB}}) \tag{B.9}$$

In clean configuration, when all the high-lift devices and the landing gear are retracted, the model makes use of 15 coefficients to calculate C_D. If the Mach number is higher or equal than the highest Mach number in clean configuration M_{max}, then the drag coefficient C_D is extrapolated using a formula dependent on M_{max}.

B.2.2. Thrust model in BADA 4

The thrust force is calculated based on the type of engine: turbofan,turboprop and piston. The turbofan and turboprop engines can be operated by either direct throttle control or a predefined setting called rating, where the following are the modelled ratings for the turbofan and turboprop engines: low idle thrust (LIDL), maximum climb thrust (MCMB) and maximum cruise thrust (MCRZ). A piston engine is typically operated only by direct throttle control.

The general formulation of the thrust force is given by Eq. (B.10), where δ is the pressure ration, W_{mref} is the weight force at the reference mass m_{ref} and C_T is the thrust coefficient.

$$T = \delta \cdot \text{W}_{\text{mref}} \cdot C_T \tag{B.10}$$

The following is the calculation of the thrust coefficient for the jet/turbofan engines for each case. For the other two engines, the physical dependencies are the same and the concept of engine rating is applicable. In the idle thrust model, the thrust coefficient depends on the Mach number and the atmospheric conditions as in Eq. (B.11), where the function f is a second order polynomial of M with coefficients that are a function of the pressure δ with four components. For the remainder of the ratings and in case the engine is operated through direct throttle input, the thrust coefficient is a function of Mach number and the throttle parameter δ_T. In this case the thrust coefficient is a fifth order polynomial of the δ_T with coefficients a fifth order polynomial of the Mach number.

$$(C_T)_{\text{idle}} = f(M, \delta) \tag{B.11}$$

$$(C_T)_{\text{gen}} = f(M, \delta_T) \tag{B.12}$$

Turbofan engines can be operated in two areas: either below a temperature deviation from ISA called the kink point or above it. The throttle parameter δ_T is function of the atmospheric conditions and Mach number in both cases, but it's either dependent a fifth order polynomial of the pressure ratio δ (below the kink point) or a fifth order polynomial of the total temperature ratio.

B.2.3. Fuel Consumption in BADA 4

The general formula for the fuel consumption F [kg s^{-1}] is calculated as function of both altitude and thrust:

$$\mathrm{F} = \delta \cdot \theta^{\frac{1}{2}} \cdot \mathrm{m_{ref}} \cdot g_0 \cdot a_0 \cdot \mathrm{L_{HV}^{-1}} \cdot C_F \tag{B.13}$$

Here, δ is the pressure ratio, θ is the temperature ratio, $\mathrm{m_{ref}}$ is the reference mass, from the PFM, a_0 is the speed of sound at sea level, $\mathrm{L_{HV}}$ is the fuel lower heating value and C_F is the fuel coefficient. The C_F is calculated differently depending on each engine type: jet, turbofan and turboprop. For turbofan and turboprop fuel models, the fuel coefficient is determined by the rating used as follows:

$$C_F = \begin{cases} (C_F)_{\mathrm{idle}}, & \text{when idle rating is used} \\ \max((C_F)_{\mathrm{gen}}, (C_F)_{\mathrm{idle}}), & \text{when non-idle rating} \\ & \text{or no rating is used} \end{cases} \tag{B.14}$$

where, $(C_F)_{\mathrm{idle}}$ is the idle thrust coefficient and $(C_F)_{\mathrm{gen}}$ is the general fuel coefficient. The former parameter is a function of Mach number and atmospheric conditions as defined by Eq. (B.15), while the later is a function of the Mach number and thrust coefficients as defined by Eq. (B.16).

$$(C_F)_{\mathrm{idle}} = f(M, .., M^2, \delta^{-1}, \sqrt{\theta}) \tag{B.15}$$

$$(C_F)_{\mathrm{gen}} = f(C_T, .., C_T^4, M, .., M^4) \tag{B.16}$$

B.3. Fuel determination process

Based on the descriptions in Appendix B.1 and Appendix B.2, it is obvious that the fuel determination process in BADA 3 and BADA 4 differ. During the simulations in BlueSky using BADA, in a level-off segment thrust T is equal to drag D, where the drag is computed using the drag coefficient C_D in Eq. (B.4). The fuel is then determined using Eqs. (B.7) and (B.8). On the other hand, the thrust in an accelerating or decelerating segment is computed based on Eq. (B.18), using a value for the longitudinal acceleration that is 80% of the maximum longitudinal acceleration for civil flights, which is independent of the aircraft type and model in BADA 3. The absolute value used to limit the true airspeed increment in longitudinal direction in the simulations is 0.5 m s^{-2}. The thrust value T, obtained using the fixed acceleration/deceleration, is compared with the maximum thrust in cruise $T_{\mathrm{max\,cruise}}$ from the Limit Model and Eq. (B.6). In case the thrust exceeds this value, the maximum thrust value is used.

$$T = D = \frac{1}{2}\rho V_{TAS}^2 S C_D \tag{B.17}$$

$$T - D = m\frac{dV_{TAS}}{dt} \tag{B.18}$$

In BADA 4, the procedure to estimate the fuel consumption in cruise flight is dependent on the type of flight segment the aircraft is on. If the aircraft is levelling-off and is flying at a constant speed, first one computes the drag using Eq. (B.3), where the drag coefficient is determined using Eq. (B.9). Then the assumption that the thrust T is equal to the D is made and the thrust coefficient C_T calculated by rearranging Eq. (B.10). Using the thrust coefficient and information on the atmospheric conditions, the fuel coefficient C_F is calculated using Eqs. (B.14) to (B.16). Once the C_F is known, the fuel consumption follows from Eq. (B.13). Then the mass of the aircraft can be updated using Eq. (B.2).

There are two ways to model an acceleration level-off segment in BADA 4: either by choosing the available engine rating (MCRZ) and computing the throttle parameter accordingly, or by choosing directly a throttle parameter value that produces a positive acceleration and a throttle coefficient that is between the $C_{T,LIDL}$ and $C_{T,MCRZ}$. Using the throttle parameter, the the thrust coefficient is determined using Eq. (B.12). The remaining of the procedure is identical to that for a constant speed segment. In the case of an deceleration segment, there is no engine rating to use, therefore a throttle parameter that produces a negative acceleration must be selected directly.

The following information is required to determine the fuel consumption in BADA 4: the aircraft model, altitude, flight phase, temperature and speed at every simulation step. This information comes from the BlueSky trajectory simulations. Since the thrust cannot be selected based on the throttle parameter in BADA

3, when using the input trajectory information to recalculate the fuel consumption using BADA 4 special attention must be payed to the throttle parameter selection. In case the aircraft is levelling-off in a constant speed segment, the thrust is computed using the nominal procedure for BADA 4 described above. However, in the case of a level-off segment in acceleration or deceleration, the throttle parameter is selected such that the acceleration or deceleration approaches the fixed value used in the simulations performed using BlueSky. In case these throttle parameters results in a thrust coefficient that is not between $C_{T,LIDL}$ and $C_{T,MCMB}$, the MCRZ engine rating is used in the case of an acceleration segment and the low idle thrust rating is used in the case of deceleration. This results in a loss of accuracy in the fuel calculation.

C

Further results

Table C.1: Mean percentage of DOTP ≤ TW over the 50 flight realisations corresponding to each fight schedule simualted with a TW type and departure delay.

		Delay				
		0 min	5 min	10 min	15 min	20 min
ADH931	**1 min**	92.0%	0.0%	0.0%	0.0%	0.0%
	strategic (TW ≤ 10 min)	100.0%	100.0%	100.0%	0.0%	0.0%
	pre-tactical (TW = 15 min)	100.0%	100.0%	100.0%	100.0%	0.0%
	60 min	100.0%	100.0%	100.0%	100.0%	100.0%
BER38A	**1 min**	98.0%	0.0%	0.0%	0.0%	0.0%
	strategic (TW ≤ 10 min)	98.0%	100.0%	100.0%	0.0%	0.0%
	pre-tactical (TW = 15 min)	98.0%	100.0%	100.0%	100.0%	0.0%
	60 min	98.0%	100.0%	100.0%	100.0%	100.0%
BER6183	**1 min**	98.0%	0.0%	0.0%	0.0%	0.0%
	strategic (TW ≤ 10 min)	98.0%	100.0%	0.0%	0.0%	0.0%
	pre-tactical (TW = 15 min)	98.0%	100.0%	100.0%	100.0%	0.0%
	60 min	98.0%	100.0%	100.0%	100.0%	100.0%
BER7LW	**1 min**	98.0%	0.0%	0.0%	0.0%	0.0%
	strategic (TW ≤ 10 min)	98.0%	100.0%	100.0%	0.0%	0.0%
	pre-tactical (TW = 15 min)	98.0%	100.0%	100.0%	100.0%	0.0%
	60 min	98.0%	100.0%	100.0%	100.0%	100.0%
CFG5KA	**1 min**	6.0%	0.0%	0.0%	0.0%	0.0%
	strategic (TW ≤ 10 min)	100.0%	100.0%	12.0%	0.0%	0.0%
	pre-tactical (TW = 15 min)	100.0%	100.0%	100.0%	12.0%	0.0%
	60 min	100.0%	100.0%	100.0%	100.0%	100.0%
CFG6KE	**1 min**	6.0%	0.0%	0.0%	0.0%	0.0%
	strategic (TW ≤ 10 min)	100.0%	88.0%	0.0%	0.0%	0.0%
	pre-tactical (TW = 15 min)	100.0%	100.0%	88.0%	0.0%	0.0%
	60 min	100.0%	100.0%	100.0%	100.0%	100.0%
DLH1831	**1 min**	94.0%	0.0%	0.0%	0.0%	0.0%
	strategic (TW ≤ 10 min)	100.0%	100.0%	100.0%	0.0%	0.0%
	pre-tactical (TW = 15 min)	100.0%	100.0%	100.0%	100.0%	0.0%
	60 min	100.0%	100.0%	100.0%	100.0%	100.0%
DLH2JW	**1 min**	0.0%	0.0%	0.0%	0.0%	0.0%
	strategic (TW ≤ 10 min)	0.0%	0.0%	0.0%	0.0%	0.0%
	pre-tactical (TW = 15 min)	100.0%	100.0%	4.0%	0.0%	0.0%
	60 min	100.0%	100.0%	100.0%	100.0%	100.0%
DLH2WA	**1 min**	72.0%	94.0%	0.0%	0.0%	0.0%
	strategic (TW ≤ 10 min)	100.0%	100.0%	100.0%	100.0%	0.0%

	pre-tactical (TW = 15 min)	100.0%	100.0%	100.0%	100.0%	100.0%
	60 min	100.0%	100.0%	100.0%	100.0%	100.0%
DLH2WT	**1 min**	52.0%	52.0%	0.0%	0.0%	0.0%
	strategic (TW ≤ 10 min)	52.0%	100.0%	50.0%	0.0%	0.0%
	pre-tactical (TW = 15 min)	52.0%	100.0%	100.0%	100.0%	0.0%
	60 min	52.0%	100.0%	100.0%	100.0%	100.0%
DLH32K	**1 min**	0.0%	0.0%	0.0%	0.0%	0.0%
	strategic (TW ≤ 10 min)	100.0%	100.0%	0.0%	0.0%	0.0%
	pre-tactical (TW = 15 min)	100.0%	100.0%	100.0%	0.0%	0.0%
	60 min	100.0%	100.0%	100.0%	100.0%	100.0%
DLH47P	**1 min**	0.0%	0.0%	0.0%	0.0%	0.0%
	strategic (TW ≤ 10 min)	0.0%	0.0%	0.0%	0.0%	0.0%
	pre-tactical (TW = 15 min)	100.0%	100.0%	0.0%	0.0%	0.0%
	60 min	100.0%	100.0%	100.0%	100.0%	100.0%
DLH4KY	**1 min**	100.0%	0.0%	0.0%	0.0%	0.0%
	strategic (TW ≤ 10 min)	100.0%	100.0%	100.0%	0.0%	0.0%
	pre-tactical (TW = 15 min)	100.0%	100.0%	100.0%	100.0%	0.0%
	60 min	100.0%	100.0%	100.0%	100.0%	100.0%
DLH65E	**1 min**	0.0%	0.0%	0.0%	0.0%	0.0%
	strategic (TW ≤ 10 min)	100.0%	100.0%	0.0%	0.0%	0.0%
	pre-tactical (TW = 15 min)	100.0%	100.0%	100.0%	0.0%	0.0%
	60 min	100.0%	100.0%	100.0%	100.0%	100.0%
DLH9EL	**1 min**	72.0%	94.0%	0.0%	0.0%	0.0%
	strategic (TW ≤ 10 min)	100.0%	100.0%	100.0%	100.0%	0.0%
	pre-tactical (TW = 15 min)	100.0%	100.0%	100.0%	100.0%	100.0%
	60 min	100.0%	100.0%	100.0%	100.0%	100.0%
EZY281K	**1 min**	0.0%	0.0%	0.0%	0.0%	0.0%
	strategic (TW ≤ 10 min)	58.0%	0.0%	0.0%	0.0%	0.0%
	pre-tactical (TW = 15 min)	100.0%	100.0%	0.0%	0.0%	0.0%
	60 min	100.0%	100.0%	100.0%	100.0%	100.0%
NLY7GC	**1 min**	78.0%	0.0%	0.0%	0.0%	0.0%
	strategic (TW ≤ 10 min)	78.0%	100.0%	86.0%	0.0%	0.0%
	pre-tactical (TW = 15 min)	78.0%	100.0%	100.0%	86.0%	0.0%
	60 min	78.0%	100.0%	100.0%	100.0%	100.0%
TRA9216	**1 min**	4.0%	0.0%	0.0%	0.0%	0.0%
	strategic (TW ≤ 10 min)	100.0%	100.0%	0.0%	0.0%	0.0%
	pre-tactical (TW = 15 min)	100.0%	100.0%	100.0%	0.0%	0.0%
	60 min	100.0%	100.0%	100.0%	100.0%	100.0%
VLG18KY	**1 min**	0.0%	0.0%	0.0%	0.0%	0.0%
	strategic (TW ≤ 10 min)	100.0%	100.0%	0.0%	0.0%	0.0%
	pre-tactical (TW = 15 min)	100.0%	100.0%	100.0%	0.0%	0.0%
	60 min	100.0%	100.0%	100.0%	100.0%	100.0%
VLG18LL	**1 min**	0.0%	0.0%	0.0%	0.0%	0.0%
	strategic (TW ≤ 10 min)	100.0%	100.0%	0.0%	0.0%	0.0%
	pre-tactical (TW = 15 min)	100.0%	100.0%	100.0%	0.0%	0.0%
	60 min	100.0%	100.0%	100.0%	100.0%	100.0%

Table C.2: Mean fuel flow kgs^{-1} over the 50 flight realisations corresponding to each fight schedule simualted with a TW type and departure delay.

		Delay				
		0	**5**	**10**	**15**	**20**
ADH931	**1 min**	0.60	0.73	0.73	0.73	0.73
	strategic (TW leq 10 min)	0.60	0.61	0.61	0.73	0.73
	pre-tactical (TW = 15 min)	0.60	0.61	0.61	0.61	0.73
	60 min	0.60	0.61	0.61	0.61	0.61
BER38A	**1 min**	0.66	0.88	0.88	0.88	0.88
	strategic (TW leq 10 min)	0.66	0.72	0.72	0.88	0.88
	pre-tactical (TW = 15 min)	0.66	0.72	0.71	0.72	0.88
	60 min	0.66	0.72	0.72	0.72	0.72
BER6183	**1 min**	0.66	0.88	0.88	0.88	0.88
	strategic (TW leq 10 min)	0.66	0.72	0.88	0.88	0.88
	pre-tactical (TW = 15 min)	0.66	0.72	0.72	0.72	0.88
	60 min	0.66	0.72	0.72	0.72	0.72
BER7LW	**1 min**	0.66	0.88	0.88	0.88	0.88
	strategic (TW leq 10 min)	0.66	0.72	0.72	0.88	0.88
	pre-tactical (TW = 15 min)	0.66	0.72	0.72	0.72	0.88
	60 min	0.66	0.72	0.72	0.72	0.72
CFG5KA	**1 min**	0.75	0.80	0.80	0.80	0.80
	strategic (TW leq 10 min)	0.68	0.68	0.80	0.80	0.80
	pre-tactical (TW = 15 min)	0.68	0.68	0.68	0.80	0.80
	60 min	0.68	0.68	0.68	0.68	0.68
CFG6KE	**1 min**	0.80	0.81	0.81	0.81	0.81
	strategic (TW leq 10 min)	0.67	0.67	0.81	0.81	0.81
	pre-tactical (TW = 15 min)	0.67	0.67	0.67	0.81	0.81
	60 min	0.67	0.67	0.67	0.67	0.67
DLH1831	**1 min**	0.65	0.79	0.79	0.79	0.79
	strategic (TW leq 10 min)	0.65	0.65	0.73	0.79	0.79
	pre-tactical (TW = 15 min)	0.65	0.65	0.65	0.70	0.79
	60 min	0.65	0.65	0.65	0.65	0.65
DLH2JW	**1 min**	0.99	1.01	1.01	1.01	1.01
	strategic (TW leq 10 min)	0.95	1.01	1.01	1.01	1.01
	pre-tactical (TW = 15 min)	0.86	0.86	0.93	1.01	1.01
	60 min	0.86	0.86	0.86	0.86	0.86
DLH2WA	**1 min**	0.63	0.77	0.82	0.82	0.82
	strategic (TW leq 10 min)	0.62	0.68	0.68	0.82	0.82
	pre-tactical (TW = 15 min)	0.62	0.68	0.68	0.68	0.82
	60 min	0.62	0.68	0.68	0.68	0.68
DLH2WT	**1 min**	0.53	0.68	0.68	0.68	0.68
	strategic (TW leq 10 min)	0.53	0.58	0.68	0.68	0.68
	pre-tactical (TW = 15 min)	0.53	0.58	0.58	0.58	0.68
	60 min	0.53	0.58	0.58	0.58	0.58
DLH32K	**1 min**	0.80	0.84	0.84	0.84	0.84
	strategic (TW leq 10 min)	0.69	0.69	0.84	0.84	0.84
	pre-tactical (TW = 15 min)	0.69	0.69	0.69	0.84	0.84
	60 min	0.69	0.69	0.69	0.69	0.69
DLH47P	**1 min**	1.03	1.04	1.04	1.04	1.04
	strategic (TW leq 10 min)	0.99	1.04	1.04	1.04	1.04
	pre-tactical (TW = 15 min)	0.90	0.90	0.96	1.04	1.04
	60 min	0.90	0.90	0.90	0.90	0.90
DLH4KY	**1 min**	0.63	0.77	0.77	0.77	0.77
	strategic (TW leq 10 min)	0.63	0.63	0.68	0.77	0.77
	pre-tactical (TW = 15 min)	0.64	0.63	0.63	0.68	0.77

	60 min	0.64	0.63	0.63	0.63	0.63
DLH65E	**1 min**	0.80	0.84	0.84	0.84	0.84
	strategic (TW leq 10 min)	0.69	0.69	0.84	0.84	0.84
	pre-tactical (TW = 15 min)	0.69	0.69	0.69	0.84	0.84
	60 min	0.69	0.69	0.69	0.69	0.69
DLH9EL	**1 min**	0.63	0.77	0.82	0.82	0.82
	strategic (TW leq 10 min)	0.62	0.68	0.68	0.82	0.82
	pre-tactical (TW = 15 min)	0.62	0.68	0.68	0.68	0.82
	60 min	0.62	0.68	0.68	0.68	0.68
EZY281K	**1 min**	0.87	0.89	0.89	0.89	0.89
	strategic (TW leq 10 min)	0.75	0.89	0.89	0.89	0.89
	pre-tactical (TW = 15 min)	0.71	0.71	0.75	0.89	0.89
	60 min	0.71	0.71	0.71	0.71	0.71
NLY7GC	**1 min**	0.76	0.91	0.91	0.91	0.91
	strategic (TW leq 10 min)	0.76	0.76	0.77	0.91	0.91
	pre-tactical (TW = 15 min)	0.76	0.76	0.76	0.77	0.91
	60 min	0.76	0.76	0.76	0.76	0.76
TRA9216	**1 min**	0.71	0.73	0.73	0.73	0.73
	strategic (TW leq 10 min)	0.63	0.63	0.73	0.73	0.73
	pre-tactical (TW = 15 min)	0.63	0.63	0.63	0.73	0.73
	60 min	0.63	0.63	0.63	0.63	0.63
VLG18KY	**1 min**	0.80	0.84	0.84	0.84	0.84
	strategic (TW leq 10 min)	0.69	0.69	0.84	0.84	0.84
	pre-tactical (TW = 15 min)	0.69	0.69	0.69	0.84	0.84
	60 min	0.69	0.69	0.69	0.69	0.69
VLG18LL	**1 min**	0.80	0.84	0.84	0.84	0.84
	strategic (TW leq 10 min)	0.69	0.69	0.84	0.84	0.84
	pre-tactical (TW = 15 min)	0.69	0.69	0.69	0.84	0.84
	60 min	0.69	0.69	0.69	0.69	0.69

Bibliography

[L1] Airbus. Global Market Forecast: Global Networks,Global Citizens 2018-2037. Technical report, AIRBUS S.A.S., Blagnac Cedex, France, 2018.

[L2] Cynthia Barnhart, Douglas Fearing, Amedeo Odoni, and Vikrant Vaze. Demand and capacity management in air transportation. *Journal on Transportation and Logistics*, 1(1-2):135–155, 2012.

[L3] Boeing. Commercial Market Outlook. Technical report, 2018.

[L4] Tatjana Bolić, Lorenzo Castelli, Luca Corolli, and Desirée Rigonat. Reducing ATFM delays through strategic flight planning. *Transportation Research Part E: Logistics and Transportation Review*, 98:42–59, 2017.

[L5] Veronica Dal Sasso, Franklin Djeumou Fomeni, Guglielmo Lulli, and Konstantinos G. Zografos. Incorporating Stakeholders' priorities and preferences in 4D trajectory optimization. *Transportation Research Part B: Methodological*, 117:594–609, 2018.

[L6] David De Smedt and Gerhard Berz. Study of the required time of arrival function of current FMS in an ATM context. *AIAA/IEEE Digital Avionics Systems Conference - Proceedings*, pages 1–10, 2007.

[L7] Jacco M Hoekstra and Joost Ellerbroek. BlueSky ATC Simulator Project: an Open Data and Open Source Approach. *7th International Conference on Research in Air Transportation*, pages 1–8, 2016.

[L8] International Civil Aviation Organisation. Time adherence in TBO. 2014.

[L9] Mihaela Mitici, Rene Verbeek, and Remon van den Brandt. Advanced prediction models for flexible trajectory-based operations. Technical Report February, ADAPT Consortium, 2019.

[L10] SESAR. The roadmap for delivering high performing aviation for Europe: European ATM Master Plan. Technical report, 2015.

[L11] F. J. van Schaik. *Introduction to Air Traffic Management*. Number August. TU Delft, 2010.